Dovepress
Taylor & Francis Group

ORIGINAL RESEARCH

Network Pharmacology and Experimental Validation of the Effects of Shenling Baizhu San, Quzhi Ruangan Fang and Gexia Zhuyu Tang on the Intestinal Flora of Rats with NAFLD

Jia Guo [1,2,]*, Anhua Shi [1,3,4,]*, Yanhong Sun[1], Shunzhen Zhang[1], Xiaoyi Feng[1,3,4], Yifan Chen[1], Zheng Yao [1,3,4]

[1]School of Basic Medical Sciences, Yunnan University of Chinese Medicine, Kunming, Yunnan, 650500, People's Republic of China; [2]Dongtai Hospital of Traditional Chinese Medicine, Dongtai, Jiangsu, 224200, People's Republic of China; [3]The Key Laboratory of Microcosmic Syndrome Differentiation, Education Department of Yunnan, Yunnan University of Chinese Medicine, Kunming, Yunnan, 650500, People's Republic of China; [4]Yunnan Key Laboratory of Integrated Traditional Chinese and Western Medicine for Chronic Disease in Prevention and Treatment, Yunnan University of Chinese Medicine, Kunming, Yunnan, 650500, People's Republic of China

*These authors contributed equally to this work

Correspondence: Zheng Yao, School of Basic Medical Sciences, Yunnan University of Chinese Medicine, Kunming, Yunnan, 650500, People's Republic of China, Tel +8618908719365, Email YaoYNUCM@163.com

Objective: In this study, we investigated the effect of Shenling Baizhu San(SLBZS), Quzhi Ruangan Fang(QZRGF) and Gexia Zhuyu Tang(GXZYT) on the intestinal flora of NAFLD rats through network pharmacology and experimental validation.

Materials and Methods: Protein-protein interaction, Gene Ontology (GO), and molecular docking were performed. Male Sprague-Dawley (SD) rats were divided into 6 groups: Normal, Model, SLBZS (7.2g/kg), QZRGF (27.72g/kg), GXZYT (28.8 g/kg) and positive control (Fenofibrate, 18mg/kg); the NAFLD model was established by High-fat diet. After one week of acclimatisation feeding consecutively, continuous gavage was given for 8 W and 12 W. Serum, liver and faeces were collected and biochemical and pathological indices were determined. The diversity and abundance of intestinal flora were also analyzed using 16S rDNA amplified sequencing.

Results: A total of 132 active ingredients were obtained from the screening results of SLBZS. A total of 202 active ingredients were obtained from the screening results of GXZYT. The screening results of QZRGF obtained 34 active ingredients. Nine common hub genes were screened from the PPI network. GO functional analysis reported that these targets were mainly closely related to the response to bacterial molecules. The molecular docking results indicated that the 11 core constituents in three compound prescriptions has good binding ability with MAPK1, AKT1, CASP3, FOS, TP53, STAT3, MAPK3.

Conclusion: The Chinese herbal compounds SLBZS, QZRGF and GXZYT may exert lipid-lowering effects through multi-components, multi-targets and multi-methods for the treatment of NAFLD while improving the diversity and abundance of the intestinal flora of the rats, and the best effect was achieved with SLBZS.

Keywords: network pharmacology, Shenling Baizhu San, Quzhi Ruangan Fang, Gexia Zhuyu Tang, NAFLD, intestinal flora

Introduction

Non-alcoholic fatty liver disease (NAFLD) is a fatty lesion of the liver caused by liver injury factors other than alcohol.[1] It has evolved from a relatively unknown disease to the most common chronic liver disease worldwide. It has been reported that nearly 25% of the global population suffers from NAFLD, which affects about 30% of the general population in Western countries.[2] NAFLD has become the number one chronic liver disease in China.[3,4] The pathogenesis of NAFLD has not yet been fully elucidated, and researchers have generally accepted the "multiple strike" theory, in

1165

Graphical Abstract
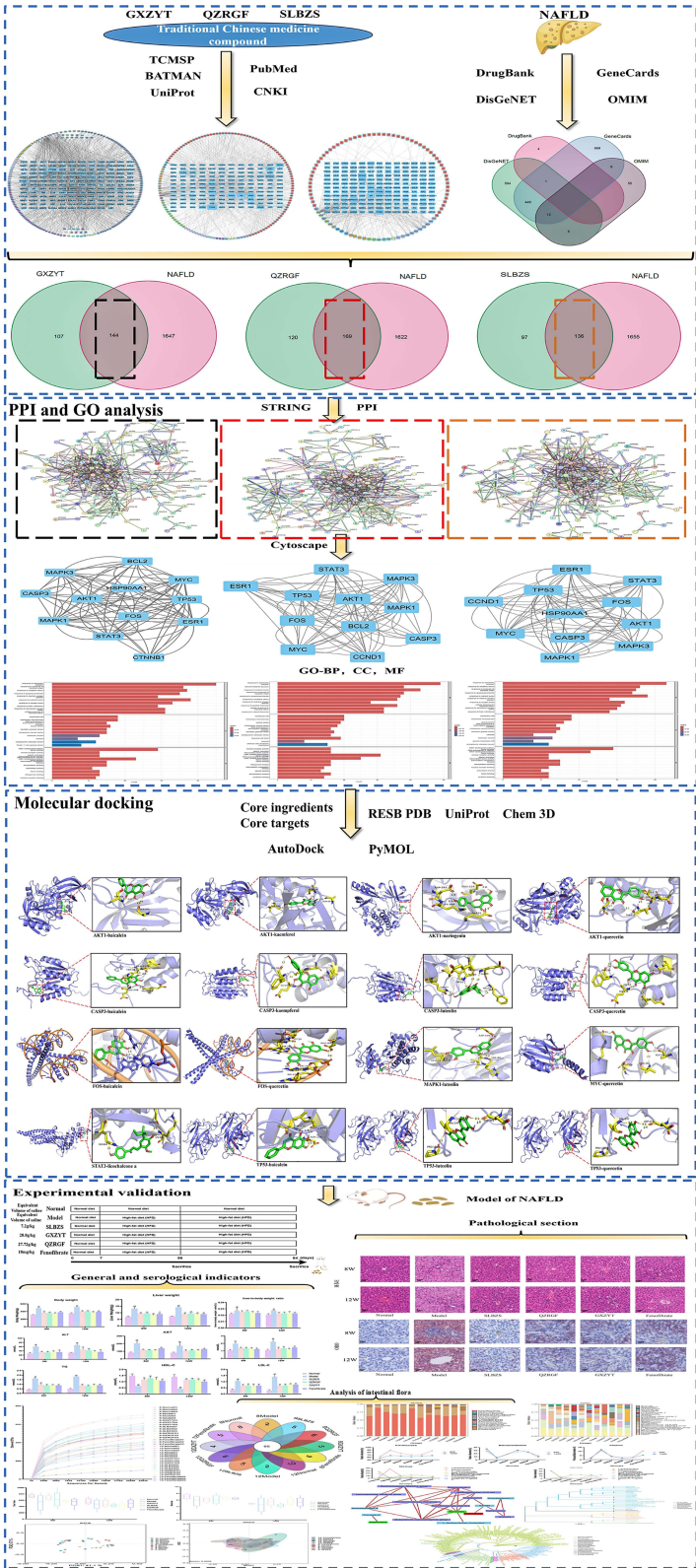
which the enterohepatic axis and innate immune disorders are the main factors. The early stage of simple hepatic steatosis is a reversible lesion, and it is the best time for pharmacological intervention.[5] NAFLD is mainly characterized by abnormal lipid metabolism, which affects the intestinal flora, and the intestinal flora also affects lipid metabolism and lipid levels, which are causative of each other.[6] There is increasing evidence that metabolic disorders caused by intestinal flora dysbiosis play an important role in the pathogenesis of NAFLD.[7] There exists an inextricable bi-directional connection between the liver and intestines in terms of anatomy and biological function, which is known as the gut-liver axis, which is consistent with the theory of "liver and intestines are connected"in traditional Chinese medicine (TCM).[8]

The liver and the large intestine are closely related anatomically, and they are interconnected through the portal venous system.[9] In embryonic origin, both originate from the foregut, which provides a structural basis for "gut and liver connectedness". Modern medicine has proposed "the gut-liver axis" theory,[10] which suggests that there is an interaction between intestinal microorganisms and the liver. Products derived from gut microbes are transported to the liver through the portal vein and influence liver metabolism through multiple pathways. Bile and antibodies from the liver can, in turn, be secreted into the intestine and influence the intestinal flora.[11,12] As an important component of the enterohepatic axis, the intestinal flora not only participates in the host's nutrient metabolism, but also maintains the functional integrity of the intestinal mucosal barrier and immune regulation.[13] The liver derives 75% of its blood supply from the portal vein, making it the first organ to be exposed to intestinal flora and metabolites via portal blood.[14] A normal intestinal barrier prevents the transfer of microorganisms and metabolites or toxins from the intestinal lumen to the extra-intestinal lumen, and disruption of the intestinal barrier may cause translocation of intestinal microorganisms, over activate the immune system, and trigger or promote the development of hepatic inflammation. Thus, the development of NAFLD can affect the homeostasis of intestinal flora, and abnormalities of intestinal flora and metabolites can also affect the development of NAFLD.[15]

Although there is an increasing amount of basic research on NAFLD, there is still a lack of specific drugs for the treatment of NAFLD.[16] In this context, it is noteworthy that the efficacy of traditional Chinese medicine (TCM) in treating NAFLD through intestinal flora is being affirmed by clinical practice and research.[17] Some studies have shown that Chinese medicine enters the digestive tract through oral intake, part of it is directly absorbed into the blood through the gastric mucosa, and the other parts with lower bioavailability are not absorbed from the upper gastrointestinal tract, reach the large intestine through the small intestine, and come into contact with intestinal flora and have interactions with each other, and the components of the effective parts of Chinese medicine not only change the metabolism of the intestinal flora, but also are transformed or metabolized by the intestinal flora.[18] Chinese medicine can also prevent the displacement of intestinal bacteria and endotoxins by regulating the intestinal flora, balancing the beneficial and pathogenic bacteria, and can significantly improve the regeneration ability of mucosal cells and reduce the excessive mucosal permeability, thus improving the barrier function of the mucosa.[19] According to TCM, NAFLD caused by long-term overeating is characterized by intestinal symptoms such as spleen deficiency, phlegm stagnation, blood stasis and diarrhea and loose stools. Modern studies have shown that intestinal flora dysfunction plays an important role in the pathogenesis of various chronic liver diseases, and the digestive symptoms are consistent with the evidence of spleen deficiency in TCM.[20]

Previous studies have shown that early NAFLD can be improved and treated by strengthening the spleen and resolving blood stasis. Shenling Baizhu San(SLBZS) is a classic formula for strengthening the spleen and eliminating dampness from the Tai Ping Hui Min He Yao Bao Fang, which has the effect of benefiting qi, tonifying the spleen, resolving dampness and stopping diarrhea. Modern pharmacological studies have confirmed that Renshen and Baizhu not only have good antibacterial, antioxidant and immune regulation effects, but also can adjust the structure of intestinal flora by reducing the number of enterococci, lowering the value of *Firmicutes / Bacteroidetes* and increasing the composition of probiotic bacteria.[21] The therapeutic effect of SLBZS on NAFLD may be related to the regulation of hepatic mitochondrial energy metabolism by intestinal flora and its metabolites, and may be associated with the UCP2/ AMPK/IF1 signaling pathway.[22] Quzhi Ruangan Fang(QZRGF) is an empirical formula of Professor Su Lian, an expert in liver diseases and an honorary famous Chinese medicine practitioner in Yunnan Province, China, which has the efficacy of softening the liver and strengthening the spleen, regulating qi and activating blood circulation. Previous

studies have demonstrated that QZRGF can improve blood lipids, liver lipids, hepatic tissue steatosis and haemorheology-related indexes in high-fat diet induced fatty liver rats.[23,24] As one of the famous formulas for removing blood stasis in Wang Qingren's "Reform and Error Correction of Medical Forests" in the Qing Dynasty, the group found that the mechanism of action of Gexia Zhuyu Tang(GXZYT) removing formula in improving lipid deposition in hepatocytes of rats with NAFLD might be related to the modulation of lipid metabolism, the reduction of the expression of CD62p, and the reduction of platelet aggregation rate.[25,26] The group's previous research on the three compound formulas found that the high-dose group had the best effect, therefore, the high-dose group was chosen for all the comparative studies in this experiment.[27–29]

The complex composition and diverse targets of TCM compounding have led to more difficulties in studying the mechanisms of TCM compounding. It was found that there are many similarities between the core concepts of TCM holistic treatment and network pharmacology.[30] So some scholars proposed the research strategy of Chinese medicine network to study Chinese medicine pharmacology.[31] In recent years, the study of network pharmacology of Chinese medicine has achieved vigorous development. It has emerged as an important intersection between TCM and network pharmacology. By exploring the mechanism of action of TCM at the molecular level and in the context of biological networks, it can provide a new way to study the mechanism of action of TCM.[32] In this study, we systematically analyzed the mechanism of action of SLBZS, QZRGF and GXZYT in the treatment of NAFLD as well as their interfering effects on the intestinal flora at the molecular level by means of network pharmacology, bioinformatics, molecular docking and other means.

Materials and Methods

Screening of Active Ingredients and Targets of Action of Shenling Baizhu San, Quzhi Ruangan Fang and Gexia Zhuyu Tang

Firstly, the active ingredients of Shenling Baizhu San, Quzhi Ruangan Fang and Gexia Zhuyu Tang were screened from the Chinese herbal tablets (https://www.example.comtcmsp.php)[33] using the criteria of Oral Bioavailability (OB) ≥ 30% and Drug Likeness (DL) ≥ 0.18. Meanwhile, with the help of Bioinformatics Analysis Tool for Molecular Mechanism of Action of Traditional Chinese Medicines (BATMAN-TCM),[34] we searched for the Chinese medicine Wulingzhi,[35] which was not available in the TCMSP platform, with the search criteria of Score ≥ 20 and P-value < 0.05 to complete the whole formula of GXZYT. Literature was searched through CNKI to find the compositional information of Lanhuasheng,[36] and the targets corresponding to the active ingredients were predicted and organized through the SwissTarget website (http://swisstargetprediction.ch/). Then, the protein targets of these screened active ingredients were retrieved in TCMSP and their chemical composition and targets were supplemented from CNKI and PubMed. Subsequently, the protein targets were entered into the UniProt database (www.uniprot.org)[37] for standardization using Homo sapiens, and the target information of all the drugs obtained earlier was annotated by means of an annotation file, which converts the full name of the gene into the symbol of the gene.

Screening for NAFLD-Related Targets

Using "NAFLD" as the keyword, potential therapeutic targets for NAFLD were explored from the databases of OMIM (https://omim.org/),[38] DrugBank (https://go.drugbank.com/),[39] DisGeNET (https://www.disgenet.org/),[40] Gene Recognition Cards (http://www.genecards.org/) databases[41] to mine potential therapeutic targets for NAFLD. Finally, the install. Packages ("venn") package was installed through R. The four database disease targets were removed from duplicate targets and concatenated sets were taken to obtain the final disease-associated genes, and the Wayne diagram was plotted.

Construction of the Relationship Between Effective Active Ingredients and NAFLD

Therapeutic targets of Shenling Baizhu San, Quzhi Ruangan Fang and Gexia Zhuyu Tang Cytoscape 3.9.1 was used to visualize the data and construct the maps of the active ingredient-NAFLD therapeutic targets of Shenling Baizhu San, Quzhi Ruangan Fang and Gexia Zhuyu Tang respectively.

Construction of a PPI Network of Effective Active Ingredients-NAFLD Targets in Shenling Baizhu San, Quzhi Ruangan Fang and Gexia Zhuyu Tang

The acquired drug-disease common target genes were inputted into the String database[42] to construct the interaction networks of Shenling Baizhu San, Quzhi Ruangan Fang and Gexia Zhuyu Tang NAFLD target proteins, respectively. Firstly, select multiple proteins, then set the biological category as "Homo Sapiens" and the interaction score as "Highest confidence > 0.9". In the network display option, we chose to hide unconnected nodes, and the rest of the settings used the system default values. The protein association score is set to 0.4, and each node represents all the proteins produced by a protein-coding locus. The colors of the lines in the graph include blue, red and yellow, which represent the evidence of gene co-evolution, gene fusion and text mining, respectively. The "string.tsv" file was downloaded to visualize and analyze the PPI network data using Cytoscape 3.9.1, and the CytoNCA plugin was used to find the core of the PPI network. The topological parameters include node connectivity, meso centrality and proximity to centrality, the larger the parameter value the closer the node is to the center of the network, indicating that the node is more critical in the network.[43,44]

Gene Enrichment Analysis

We used the R language in combination with the gene data analysis tools provided by Bioconductor to perform gene enrichment analysis. Specifically for Gene Ontology (GO) enrichment, the GO enrichment analysis includes three aspects: cellular component (CC), molecular function (MF) and biological process (BP). The results of all GO enrichment analyses performed were determined by $P < 0.05$.

Molecular Docking Validation

Based on these analyses, molecular docking of the core target and the main active ingredient was performed. The 3D crystal structures of the target proteins were obtained in the Protein Data Bank (PDB) (https://www.rcsb.org/).[45] Their PDB format files were downloaded, dehydrated and hydrogenated in AutoDockTools (version: 1.5.7) (https://ccsb.scripps.edu/mgltools/downloads/),[46] and then selected as a receptor and saved as a pdbqt file. The mol 2 file of the active component was obtained via TCMSP database and the chemical structure of the active ingredient was obtained in PubChem database, hydrogenated in AutoDockTools, selected as a ligand and exported as a pdbqt file. Molecular docking was performed by AutoDock (version: 1.5.7)[47] to obtain the affinity of each component for the target. Active ingredients and targets with good binding activity were screened based on affinity and visualised by PyMOL (version: 2.4.0) (http://www.pymol.org/pymol).

Preparation of Drugs

The formula "Shenling Baizhu San" is derived from the book "Taiping Huimin Hejiaobu Fang" and is composed as follows: 12g of Dangshen, 12g of Baizhu, 15g of Fulin, 15g of Baibiandou, 15g of Yiyiren, 15g of Shanyao, 10g of Chenpi, 10g of Sharen, 12g of Lianzi, 10g of Jiegeng, 6g of Gancao. SLBZS (Production batch number: 23101056) from Beijing Tong ren tang, a well-known brand of traditional Chinese medicine, was selected for this study. SLBZS routine daily dose for adults 20g. The dosage of the drug is based on the clinical equivalent dose and the body surface area of human and rats. The daily adult dosage was about 20g. Based on the clinical equivalent dose, the daily requirement of Shenling Baizhu San per 200g of rat is 20×0.018×5 = 1.8g/kg. Our previous study[27] found that a high dose was the most effective in the treatment of NAFLD, and the high dose was four times the equivalent dose (7.2 g/kg), so we chose a high dose for the experiment this time.

Gexia Zhuyu Tang: Wulingzhi 9g, Danggui 9g, Chuanxiong 6g, Taoren 9g, Danpi 6g, Chishao 6g, Wuyao 6g, Yanhuosuo 3g, Gancao 9g, Xiangfu 3g, Honghua 9g, Zhike 5g. The daily dosage for adults is about 80 g. Based on the clinically equivalent dose, the daily requirement of GXZYT per 200 g of rat is 80×0.018 × 5 = 7.2 g/kg. Our previous study[28] found that the high dose, which was four times the equivalent dose (28.8 g/kg), was the most effective in treating NAFLD, so we chose the high dose for this experiment.

Quzhi Ruangan Fang is mainly composed of 15g of Lanhuashen, 15g of Ezhu, 15g of Baizhu, 15g of Shanzha, 10g of Juhua, 6g of Qingpi and 3g of Sanqi. Sanqi is Saned into fine San and added into the formula when used. The minimum clinical dosage of the formula for human is 77g, 77×0.018 × 5 =6.93 g/kg. The high dose, which was four times the equivalent dose (27.72 g/kg), was the most effective in treating NAFLD.[29]

Fenofibrate capsules are 200mg daily for adults, Also converted from clinically equivalent doses, therefore the daily dose for rats is 200×0.018×5 =18mg/kg by gavage. Purchased from French pharmaceutical company RECIPHARMFONTAINE. Production batch number: 33145.

Raw herbs were purchased from the pharmacy of Yunnan Provincial Hospital of Traditional Chinese Medicine. The above prescriptions of QZRGF and GXZYT were boiled in the Pharmacy Department of Yunnan Provincial Hospital of Traditional Chinese Medicine and made into extracts in strict accordance with the production standards for in-hospital preparations. The extracts were cooled and stored at 4 °C. When used, the extracts were prepared with saline according to the concentration of the SLBZS, QZRGF, GXZYT and fenofibrate required for each group and the weight of the rats.

The identification of the Shenling Baizhu San, Gexia Zhuyu Tang, Quzhi Ruangan Fang components were outsourced to Wuhan metware Metabolic Biotechnology Co. (Figure 1)
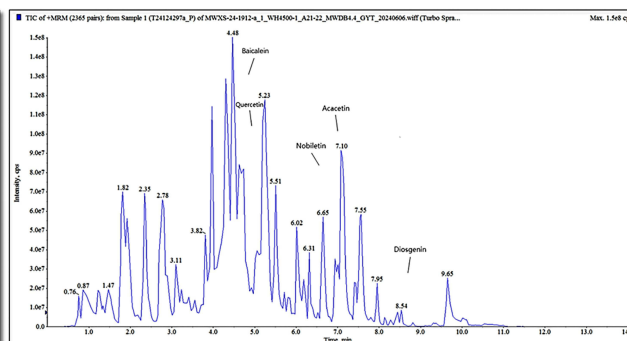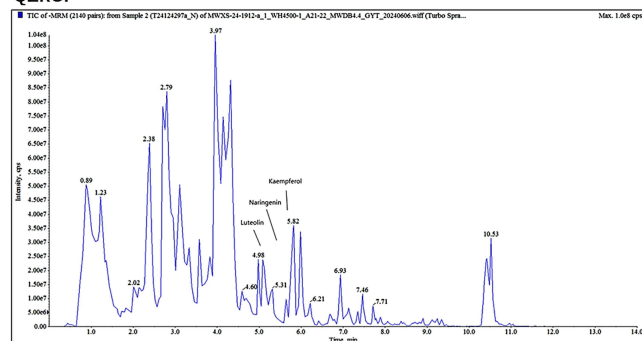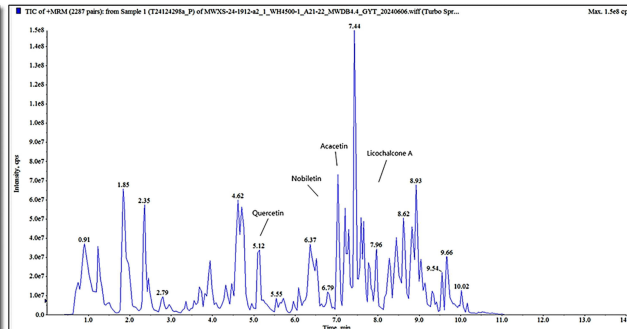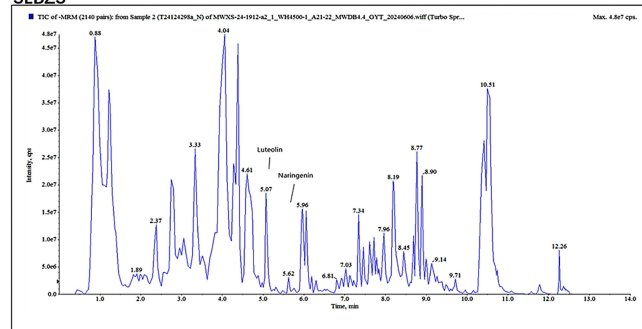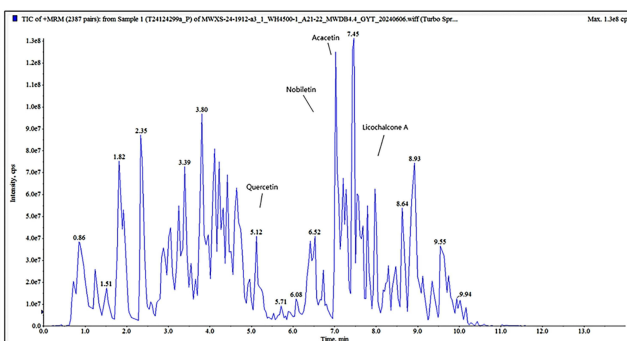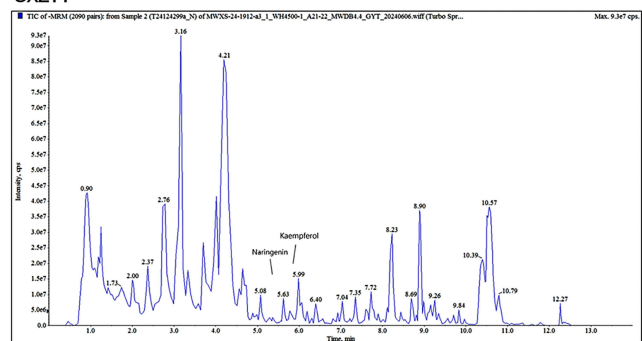

Figure 1 HPLC Chromatogram.

Co-Detection of Active Ingredients in Shenling Baizhu San, Gexia Zhuyu Tang, Quzhi Ruangan Fang Based on UPLC-MS/MS Detection Platform and Self-Constructed Database

Dry Sample Extraction

(1) Biological samples were placed in a lyophiliser (Scientz-100F) for 63h of vacuum freeze-drying;

(2) Grinding (30 Hz, 1.5 min) to powder form using a grinder (MM 400, Retsch);

(3) Use an electronic balance (MS105DM) to weigh 50 mg of sample powder, add 1200 μL of −20 °C pre-cooled 70% methanol water internal standard extract (less than 50 mg according to the proportion of every 50 mg of sample to add 1200 μL of extractant), the internal standard extract was prepared as 1 mg of standard dissolved in 1 mL of 70% methanol water to formulate 1000 μg / mL standard The internal standard extract was prepared by dissolving 1 mg of standard in 1 mL of 70% methanol water to make 1000 μg/mL standard mother liquor, and the 1000 μg/mL mother liquor was further diluted with 70% methanol to make 250 μg/mL internal standard solution;

(4) Vortex every 30 minutes, each lasting 30 seconds, for a total of 6 vortexes;

(5) After centrifugation (12000 rpm, 3 min), the supernatant was aspirated and the sample was filtered through a microporous filter membrane (0.22 μm pore size) and stored in the injection vial for UPLC-MS/MS analysis.

Chromatography and Mass Spectrometry Acquisition Conditions

The data acquisition instrumentation consists primarily of Ultra Performance Liquid Chromatography (UPLC) (ExionLC™ AD, https://sciex.com.cn/) and Tandem mass spectrometry (MS/MS).

Liquid phase conditions mainly include:

(1) Column: Agilent SB-C18 1.8 μm, 2.1 mm * 100 mm;

(2) Mobile phase: ultra-pure water (with 0.1% formic acid added) for phase A, and acetonitrile (with 0.1% formic acid added) for phase B. The mobile phase was 0.00 min and the elution gradient was 0.00 min.

(3) Elution gradient: the proportion of phase B was 5% at 0.00 min, the proportion of phase B increased linearly to 95% within 9.00 min and was maintained at 95% for 1 min, and the proportion of phase B decreased to 5% from 10.00 to 11.10 min and equilibrated at 5% for 14 min;

(4) Flow rate 0.35 mL/min; column temperature 40°C; injection volume 2 μL.

Animal Models

120 male SD rats of SPF grade, weighing 180–220g, were kept in the animal room of Yunnan University of Traditional Chinese Medicine. Production license number: SCXK (Beijing) 2019–0010, Number of Experimental Facilities Certification: SYXK(Yunnan)K2022-0004. The rats were purchased from SPF(Beijing)biotechnology co.,Ltd. All rats were given free access to feed and water throughout the experimental period at a controlled temperature of 21°C±2°C and a 12-hour light/dark cycle. (Normal feed: 29% primary secondary flour, 4.1% high gluten flour, 40.8% puffed corn, 2% fishmeal, 16% 46 soybean meal, 2% soybean oil, 6% premixes, which were purchased from SPF(Beijing)biotechnology co.,Ltd Production batch number: 06148H06152133C). High fat feed: 78.8% basal feed + 10% lard + 10% egg yolk powder + 1% cholesterol + 0.2% sodium cholate, which were purchased from SPF(Beijing)biotechnology co,Ltd. After one week of normal feeding, the experimental rats were randomly divided into 6 groups, Normal (n=10), Model (n=10), GXZYT (n=10), SLBZS (n=10), QZRGF (n=10), Fenofibrate (n=10). After 6 weeks of modeling, the livers of rats in the model group were taken for paraffin section HE and oil red O staining to observe the degree of hepatocellular steatosis. If the number of fat vacuoles in the liver cells observed on the pathological section accounts for one-third or more of the field of view, it indicates successful modeling. After the success of modeling was confirmed, the amount of drug administered to each rat was calculated according to the body weight of the rats, and the drug was diluted and dissolved in physiological saline. SLBZS, GXZYT, QZRGF, and Fenofibrate groups of rats were orally administered with a drug volume of 18mg/kg, respectively. The normal group and model group were orally administered with 2mL/d

physiological saline. This study was approved by the Animal Ethics Committee of Yunnan University of Traditional Chinese Medicine (Ethics Committee approval number: R-062021LH013).

Sample Preparation

On the day before euthanasia, we collected fecal samples for 16S rDNA sequencing. After the last administration, fasted for 12 hours and the rats were anesthetized by intraperitoneal injection of 3% pentobarbital (0.1 mL/100 g body weight). The entire livers were excised and stored at - 80°C for histological content analysis. Blood was taken from the abdominal aorta, and the whole blood was centrifuged at 3000×g at 4°C for 15 min, and the supernatant was collected and dispensed into 1.5 mL centrifuge tubes and stored at - 20°C for biochemical analysis.

Biochemical Analysis

A Roche automatic biochemical analyzer (Roche, Switzerland; model: Cobas c311) and Biochemical test kits (Nanjing Jiancheng Bioengineering Company) were used. Blood was taken from the abdominal aorta of rats, and venous blood and whole blood were collected. It was left for about 2 h, centrifuged at 3000 rpm for 15 min, and the supernatant was taken to evaluate the liver function and lipid indexes, including ALT, AST, TC, TG, high-density lipoprotein cholesterol (HDL-C), and low-density lipoprotein cholesterol (LDL-C). Each step was performed according to the instructions of the kit.

Pathological Examination of the Liver

Livers were fixed with tissue fixative for >24 hours, then removed, dehydrated and embedded, cut into two 5×5 × 2 cm cubes and stained with H&E staining in paraffin sections and O staining in frozen sections according to the instructions of the staining kit, each of which was about 5 μm in thickness. Finally, the membrane was sealed with gelatine, and the histopathological changes of the liver specimens were observed under the microscope and calculated lipid volume fraction (lipid area/total area×100%).

Detection of Bacterial Diversity and Abundance in Rat Feces Faeces

We collected rat feces, transferred them to sterile eppendorf (EP) tubes, froze them in liquid nitrogen and stored them at - 80°C. Stored intestinal contents were sent on dry ice to GemVision in Suzhou, China for testing. Construction of high-throughput sequencing libraries and sequencing based on the Illumina MiSeq platform were performed by GENEWIZ (Suzhou, China). DNA was extracted using the Magen Hipure Soil DNA Kit following the instructions for use. We used a Qubit 2.0 Fluorometer (Invitrogen, Carlsbad, CA) to detect the concentration of DNA samples, and the MetaVx™ Library Construction Kit (GENEWIZ, Inc., South Plainfield, NJ, USA) to construct sequencing libraries. The two highly variable regions of prokaryotic 16S rDNA, including V3 and V4, were amplified using a series of PCR primers designed by GemViz using 30–50ng of DNA as template according to the manufacturer's instructions. The two highly variable regions including V3 and V4 on prokaryotic 16S rDNA were amplified using a series of PCR primers designed by Viwit Jin as a template of 30–50ng DNA. The upstream primer containing the sequence "CCTACGGRRBGCASCAGKVRVGAAT" and the downstream primer containing the sequence "GGACTACNVGGGGTWTCTAATCC" were used to amplify the V3 and V4 regions. In addition, the PCR product of 16S rDNA was spliced by PCR with an Index at the end for NGS sequencing. Library quality was checked using an Agilent 2100 Bioanalyzer (Agilent Technologies, Palo Alto, CA, USA) and library concentration was checked using a Qubit2.0 Fluorometer (Invitrogen, Carlsbad, CA). After DNA library mixing, PE250/300 double-end sequencing was performed according to the Illumina MiSeq (Illumina, San Diego, CA, USA) instrument instruction manual, and the sequence information was read by MiSeqControlSoftware (MCS), which comes with the MiSeq.[48–51]

Statistical Analysis

Data were statistically analyzed using SPSS 26.0 software, and the measurement information was expressed as the mean and standard deviation $\bar{x} \pm s$. Firstly, the variance of the data in each group was tested for chi-square, one-way ANOVA was performed for chi-square between groups, and the two comparisons were made using the LSD test; if the variance

was not chi-square, the rank-sum test was used, and the two comparisons were made using the Dunnett's T3 test. The test level was α=0.05. GraphPad Prism 9.0 was used to draw the images.

Results
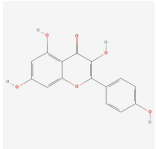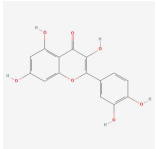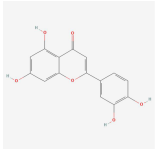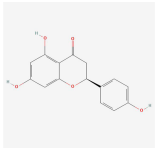
Network Pharmacology Analysis

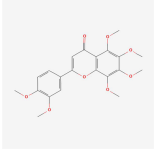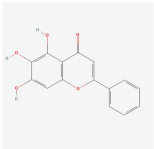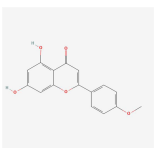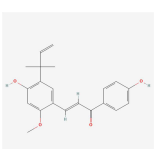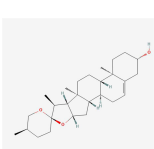### Active Ingredients and Targets of SLBZS, GXZYT and QZRGF

A total of 132 active components were isolated from SLBZS, including 1 Baibiandou, 3 Baizhu, 4 Fulin, 83 Gancao, 4 Jiegeng, 9 Lianzi, 16 Renshen, 9 Shanyao, 4 Sharen, and 5 Yiyiren; among them, 6 components were shared. A total of 34 active ingredients were isolated from QZRGF, including 3 from Baizhu, 1 from Ezhu, 16 from Juhua, 3 from Qingpi, 5 from Sanqi, 2 from Shanzha, and 4 from Lanhuasheng. 272 active ingredients were isolated from GXZYT, including 2 from Danggui, 23 from Taoren, 22 from Honghua, and 22 from Xiangfu. Honghua 22, Xiangfu 18, Wuyao 9, Danpi 11, Chishao 29, Chuanxiong 7, Yanhusuo 49, Zhike 5, Wulingzhi 6, Gancao 92. (See Table 1)

Table 1 Traditional Chinese Medicines and Main Active Ingredients of SLBZS, GXZYT and QZRGF

MOL ID	Molecule Name	Structure	OB (%)	DL	Source
MOL000422	Kaempferol		41.88	0.24	Renshen, Juhua, Shanzha, Honghua, Xiangfu, Danpi, Gancao
MOL000098	Quercetin		46.43	0.28	Honghua, Wuyao, Danpi, Gancao, Yanhusuo, Lianzi, Shanzha, Juhua, Sanqi
MOL000006	Luteolin		36.16	0.25	Xiangfu, Lianzi, Jiegeng, Juhua, Honghua
MOL004328	Naringenin		59.29	0.21	Juhua, Qingpi, Gancao, Zhike,

(Continued)

Table 1 (Continued).

MOL ID	Molecule Name	Structure	OB (%)	DL	Source
MOL005828	Nobiletin		61.67	0.52	Qingpi, Zhike
MOL002714	Baicalein		33.52	0.21	Honghua, Chishao
MOL001689	Acacetin		34.97	0.24	Jiegeng, Juhua
MOL000497	Licochalcone a		40.79	0.29	Gancao
MOL000546	Diosgenin		80.88	0.81	Shanyao

NAFLD Disease Target Genes Combined with Drug Target Genes of SLBZS, GXZYT and QZRGF

Nonalcoholic fatty liver disease (NAFLD) targets were screened with the keyword "Nonalcoholic fatty liver disease" from GeneCards, OMIM, Drug Bank, and DisGeNET databases, and median values were screened, and a total of 1792 NAFLD-related disease genes were obtained by running a concatenation operation in R version 4.2.0 software, a total of 1792 disease genes associated with NAFLD were obtained (Figure 2A). In further studies, a total of 4982 TCM target genes for GXZYT were obtained from TCMSP and BATMAN-TCM databases, and 251 non-duplicated TCM target genes were obtained after de-duplication. Comparing these TCM target genes with NAFLD-related disease genes, 144 intersecting genes were obtained. A total of 2416 TCM target genes of SLBZS were obtained from TCMSP database, and 233 non-duplicated TCM target genes were obtained after de-duplication. Comparing these TCM target genes with
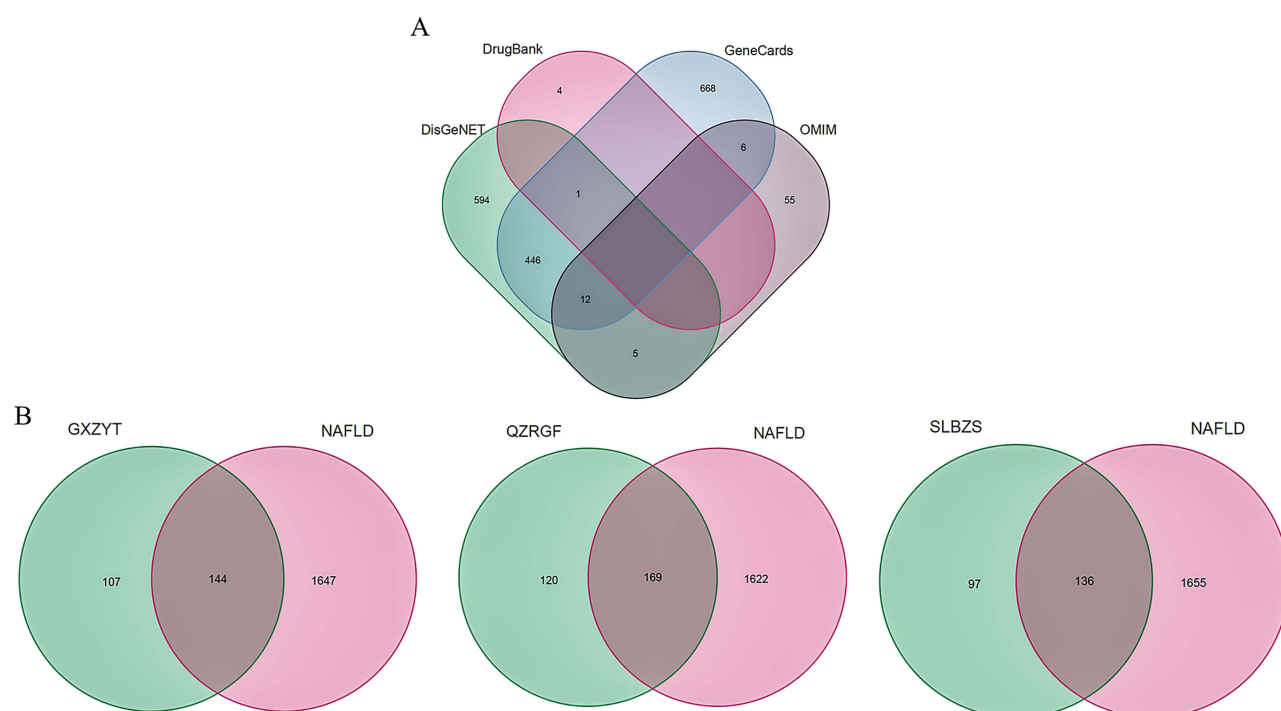
Figure 2 (**A**) NAFLD-related disease genes (**B**) Intersection of GXZYT, QZRGF and SLBZS Chinese medicine target genes and NAFLD disease genes.

NAFLD-related disease genes, 136 intersecting genes were obtained. A total of 1144 TCM target genes of QZRGF were obtained from the TCMSP database and CNKI literature. After deduplication, 289 non repetitive traditional Chinese medicine target genes were obtained. Comparing these TCM target genes with NAFLD-related disease genes, 169 intersecting genes were obtained (Figure 2B).

Graph of SLBZS, GXZYT and QZRGF Effective Active Ingredients-NAFLD Therapeutic Target Modulation Relationship

Cytoscape 3.9.1 software was used to construct the regulatory network of Chinese medicine compound and analyze the active ingredients and NAFLD disease-related genes of SLBZS, GXZYT and QZRGF. In the GXZYT active ingredient NAFLD network, Yanhusuo was identified by purple, Xiangfu was identified by light purple, Wuyao was identified by pink, Taoren was identified by dark yellow, Honghua was identified by light grey, Chuanxiong was identified by light yellow, Chishao was identified by green, Danpi was identified by red, Zhike was identified by light green, Gancao was identified by grey, Danggui was identified by green, and Wulingzhi was identified by yellow. In the overlapping colours, the main drugs associated with NAFLD treatment in GXZYT are Honghua, Xiangfu, Gancao and Zhike. In the QZRGF active active ingredient-NAFLD network, Lanhuashen is identified in red, Sanqi in yellow, Shanzha in green, Baizhu in blue, Ezhu in light yellow, Juhua in purple, and Qingpi in dark blue. In the overlapping colours, the main drugs associated with NAFLD treatment in QZRGF are Lanhuashen, Juhua and Sanqi. In the SLBZS active active ingredient-NAFLD network, Renshen is identified in green, Shanyao is identified in pink, Sharen is identified in grey, Yiyiren is identified in purple, white Baibiandou is identified in blue, Baizhu is identified in light yellow, Fulin is identified in light purple, Gancao is identified in red, Jiegeng is identified in blue, and Lianzi is identified in yellow. In the overlapping colors, the main drugs associated with NAFLD treatment in SLBZS are Renshen, Shanyao, Gancao and Lianzi. Node size indicates the degree of relevance (Figure 3).

Protein Interaction Networks (PPI)

The common targets of SLBZS, GXZYT and QZRGF were imported into the STRING database and analyzed to obtain the PPI network diagrams (Figure 4A). The PPI network graphs were imported into Cytoscape 3.9.1 software for
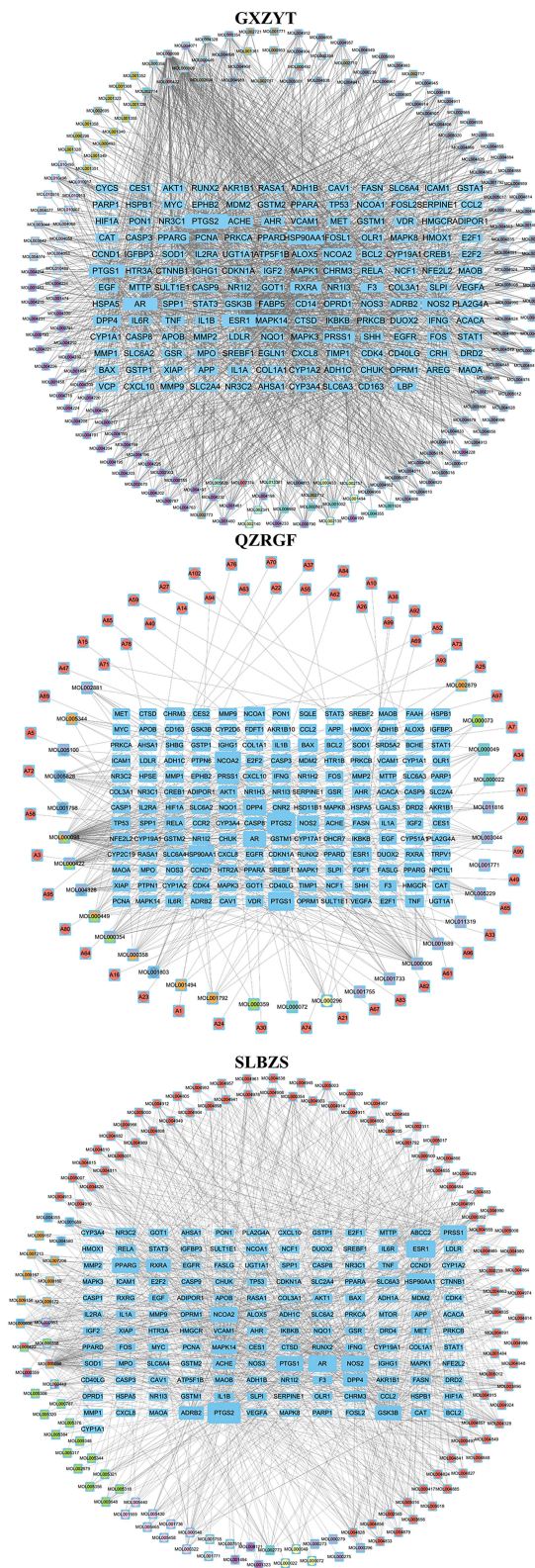
Figure 3 Effective active ingredients of GXZYT, QZRGF and SLBZS-NAFLD treatment target regulatory network diagram.
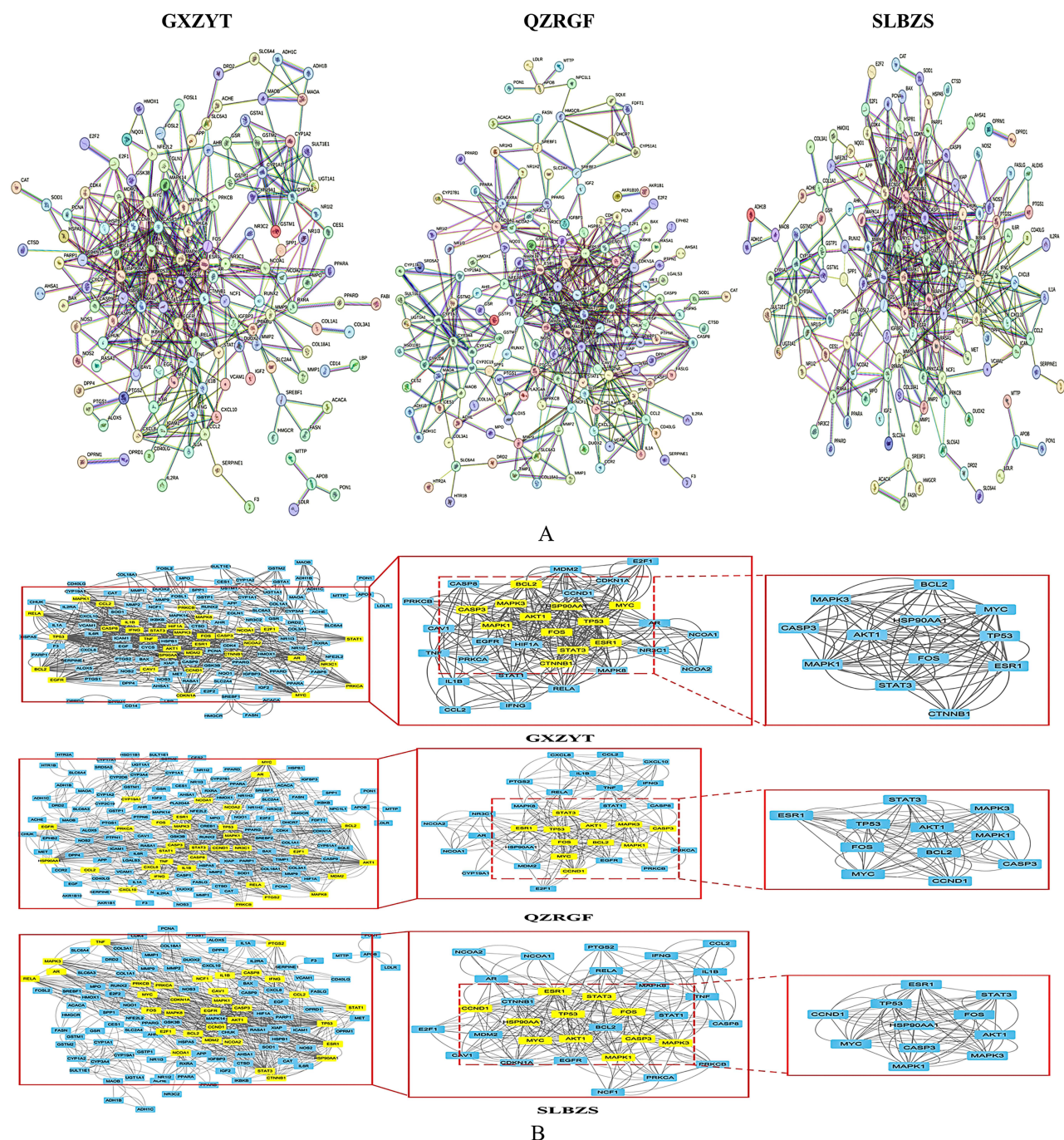
Figure 4 (**A**) Network map of protein interactions between GXZYT, QZRGF and SLBZS targets and NAFLD disease genes (**B**) Treatment of NAFLD target PPI networks using STRING's GXZYT, QZRGF and SLBZS. And use Cytoscape to treat the PPI network and get the PPI network core targets.

visualization and analysis, "Degree", "Eigenvector", "LAC" and "Network". "The core targets of SLBZS were CCND1, MAPK1, AKT1, CASP3, HSP90AA1, FOS, ESR1, TP53, STAT3, MAPK3, MYC, and GXZYT were MAPK1, AKT1, CASP3, FOS, MAPK3, MYC, CASP3, FOS, HSP90AA1, BCL2, ESR1, TP53, STAT3, MAPK3, CTNNB1, MYC. The core targets of QZRGF are: BCL2, TP53, ESR1, STAT3, MAPK3, FOS, MYC, CCND1, MAPK1, AKT1, CASP3. The three party intersection targets of the core targets were MAPK1, AKT1, CASP3, FOS, ESR1, TP53, STAT3, MAPK3, MYC. (Figure 4B)

GO Enrichment Analysis

The tripartite and NAFLD co-targets were introduced into Cytoscape and subjected to GO enrichment and KEGG pathway analysis via R language. The analysis results demonstrated GO enrichment results at three levels: biological process (BP), molecular function (MF) and cellular composition (CC). The results of the study showed that by treating NAFLD with SLBZS, GXZYT and QZRGF, respectively, we found that we could modulate the response to xenobiotic stimulus, response to oxidative stress, response to molecule of bacterial, originate response to lipopolysaccharide, and many other biological processes. The results ranked according to the *P* value from smallest to largest showed that Diaphragm Downward Expelling Blood Stasis Tang was closely related to response to molecule of bacterial in the treatment of NAFLD. The relationship is close (Figure 5).

Molecular Docking Validation

Based on the above analysis, 9 core components (baicalein, luteolin, nobiletin, quercetin, kaempferol, naringenin, licochalcone a, diosgenin, the acacetin) were molecularly docked with core targets of MAPK1, AKT1, CASP3, FOS, TP53, STAT3, and MYC (Table 2 and Figure 6). Affinity $< −4.25$ kcal-mol-1 indicates the presence of binding activity between the ligand and the target; affinity $< −5.0$ kcal-mol-1 indicates good binding activity; affinity $< - 7.0$ kcal-mol-1 indicates strong docking activity.[52] The best docking activities were screened at AKT1-diosgenin (−9.51), AKT1-beta-carotene (−9.99), AKT1-baicalein (−7.6), TP53-baicalein (−8.41), TP53-luteolin (−8.48), TP53- quercetin (−8.33), TP53-nobiletin (−7.99), TP53-acacetin (−6.61), CASP3-luteolin (−7.11), CASP3-baicalein (−6.7), FOS-quercetin (−6.44), STAT3-licochalconea (−5.89), MAPK1-Chryseriol (−6.66), MAPK1-chryseriol (−6.66), and MAPK1-chryseriol (−6.66), MAPK1-isorhamnetin (−6.68), MYC-quercetin (−6.17).

Animal Experiment Verification

The SLBZS, QZRGF and GXZYT All Reduced Lipid Deposition and Liver Injury in Rats with NAFLD

We gave the rats in the Normal group a normal diet, the Model, SLBZS, QZRGF, and GXZYT groups were given a high-fat diet, the Normal and Model groups were given an equal amount of saline, and the TCM groups were given their respective TCM compounds, which were taken at 8W and 12W, respectively (Figure 7A). The body weight and liver weight of rats in the Model group were significantly higher than those in the normal group ($P< 0.01$). Compared with the model group, the body weight and liver weight of rats in all dosing groups were significantly lower ($P< 0.01$). The liver-to-body ratio of rats in the Model group was significantly higher than that of the normal group ($P< 0.01$), and the liver-to-body ratios of rats in all groups were significantly lower than that of the model group ($P< 0.01$; Figure 7B–D). Compared with the normal group, serum ALT and AST levels of rats in the Model group were significantly higher ($P< 0.01$). Compared with the Model group, ALT and AST levels of rats in the Fenofibrate group were significantly lower ($P< 0.01$). AST and ALT levels of rats in the SLBZS, QZRGF and GXZYT groups were significantly lower ($P< 0.01$) (Figure 7E and F). As for lipid levels, compared with the normal group, serum TC, TG and LDL-C levels were significantly higher and HDL-C levels were significantly lower in the Model group of rats ($P< 0.01$). Compared with the Model group, the serum TC, TG and LDL-C levels of rats in each administration group were significantly reduced, and the HDL-C level was significantly increased ($P< 0.01$) (Figure 7G–J). HE staining results (Figure 7K) showed that the liver of rats in the Normal group had an intact histological structure, and the hepatocytes were arranged in strips radially outward around the central vein. In contrast, rats in the Model group showed a large number of microvesicular and macrovesicular steatosis in the hepatocytes, severe damage to the lobular structure, ballooning hepatocytes. The area of fatty vacuoles and balloon-like lesions in the hepatocytes of rats in the herbal and fenofibrate groups was significantly reduced compared with the model group. The best effect was observed in the GXZYT group, which made the liver basically return to the normal level. The results of oil red O staining showed that the liver cells of rats in the Normal group had a clear and complete liver structure, the nuclei of the cells showed blue-purple color, and there was no deposition of red lipid droplets in the cytoplasm; the rats in the Model group had a large number of red lipid droplets were aggregated. The lipid droplets in the administered group were significantly reduced, the reddened area of liver tissue was reduced, and the liver was basically restored to the normal level. This indicated that all groups of herbal compound could reduce hepatic steatosis and liver injury (Figure 7L).
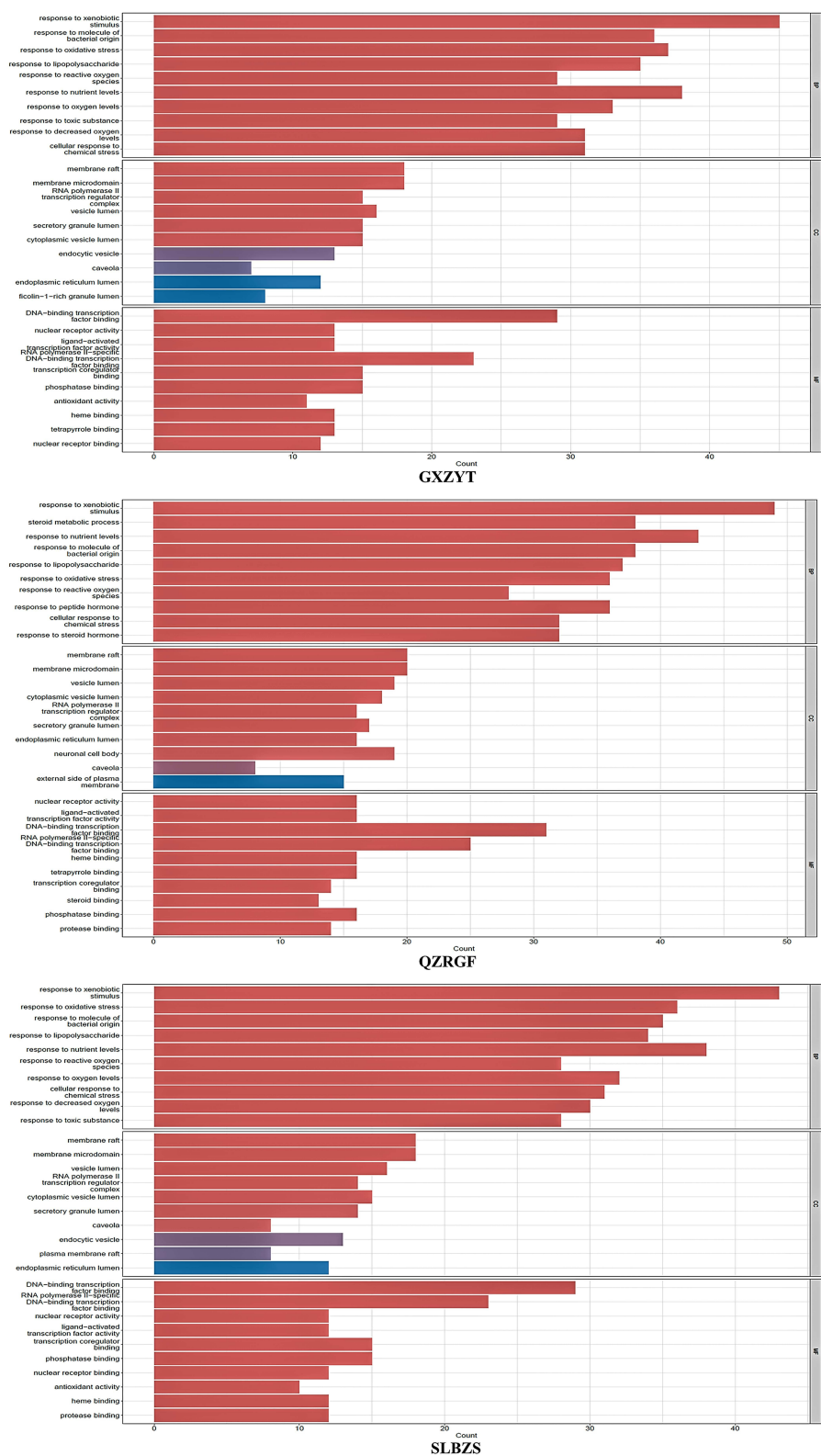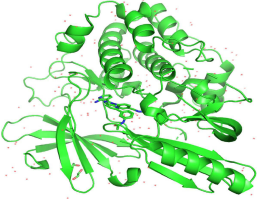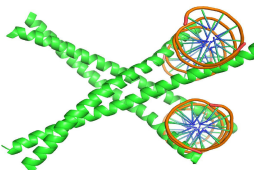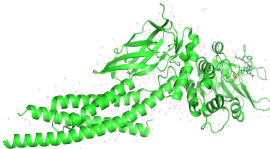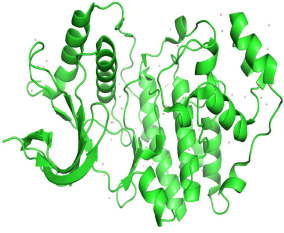
Figure 5 GO enrichment analysis: top 10 *P* values for Biological process(BP), Cellular component(CC) and Molecular function(MF).

Table 2 Molecular Docking Information of Core Components and Core Targets

NO	Protein	PDB ID	Structure	Docking Compound	Affinity (kcal/mol)
1	AKT1	4EJN		Diosgenin kaempferol luteolin naringenin quercetin	−9.51 −7.38 −7.48 −6.2 −7.4
2	CASP3	1GFW		Baicalein kaempferol luteolin naringenin quercetin acacetin	−6.7 −6.59 −7.11 −5.92 −6.66 −6.88
3	FOS	1FOS		Baicalein quercetin	−6.44 −6.44
4	STAT3	6NJS		Licochalconea	−5.89
5	TP53	5AOI		Baicalein luteolin nobiletin quercetin acacetin	−8.41 −8.48 −7.99 −8.33 −6.61

(*Continued*)

Table 2 (Continued).

NO	Protein	PDB ID	Structure	Docking Compound	Affinity (kcal/mol)
6	MAPK1	7E75		Licochalconea luteolin naringenin quercetin Artemetin Chryseriol isorhamnetin	−6.5 −6.63 -6.29 −6.76 −6.05 −6.66 -6.68
7	MYC	8J2Q		Quercetin	−6.17

The Tripartite Formulae of SLBZS, QZRGF and GXZYT Can Improve the Flora Structure of Rats with NAFLD

In order to investigate the effect of tripartite on the diversity of rat intestinal flora, fecal 16S rDNA sequencing was used to compare the diversity of rat intestinal flora after herbal medicine intervention, including alpha diversity analysis and beta diversity analysis. The community richness dilution curve showed that the sequencing amount covered all the intestinal flora in the samples, which met the requirements of data analysis. (As shown in Figure 8A), each curve represents one sample, marked with different colors; the number of OTUs increased with increasing sequencing depth. The dilution curves of each group of rat intestinal flora firstly increased and then flattened out, ie, more data volume would only produce a very small number of new species, indicating that the sequencing depth was sufficient to meet the requirements of data analysis. Based on the results of OTU clustering analysis, we counted the OTUs common and specific to the identified microbial species in each group of rat fecal samples and plotted the petal diagrams in (Figure 8B). A total of 188 different bacterial species were identified, of which 64 strains were specifically identified in each group. 95 species were common to the 12 groups of rats, as shown in Figure 8B. The intestinal microorganisms in the fecal isolates of rats in each group were rich in species. Compared with the Normal group, there was a significant decrease in the bacterial species in the Model group and a significant increase in all bacterial species in the medicated group. Compared with the Normal group, the Chao1 index of intestinal contents decreased in the Model group, and increased in the GXZYT, QZRGF, SLBZS, and Fenofibrate groups, with the most significant improvement in the flora of the SLBZS group, followed by the GXZYT and QZRGF groups in the 8-week period, and in the 12-week period, the most significant improvement in the flora of the GXZYT group, followed by the SLBZS and QZRGF groups in the 12-week period. SLBZS and QZRGF groups (Figure 8C) Compared with the Normal group, the Shannon index of the intestinal contents of the rats in the Model group was reduced, and the GXZYT, QZRGF, SLBZS and Fenofibrate groups showed an increasing trend, and the most significant improvement in the flora was observed in the SLBZS group followed by the QZRGF and GXZYT groups among the 8-week groups. The most significant improvement of the flora was observed in the QZRGF and GXZYT groups among the 12-week groups. QZRGF group showed the most significant improvement in flora, followed by SLBZS and GXZYT groups (Figure 8D). The β-diversity analysis of intestinal flora was performed using the Unifrac distance method, which calculates the distance between samples and compares the magnitude of the differences in species diversity between samples and groups. PCA analysis revealed that the intestinal
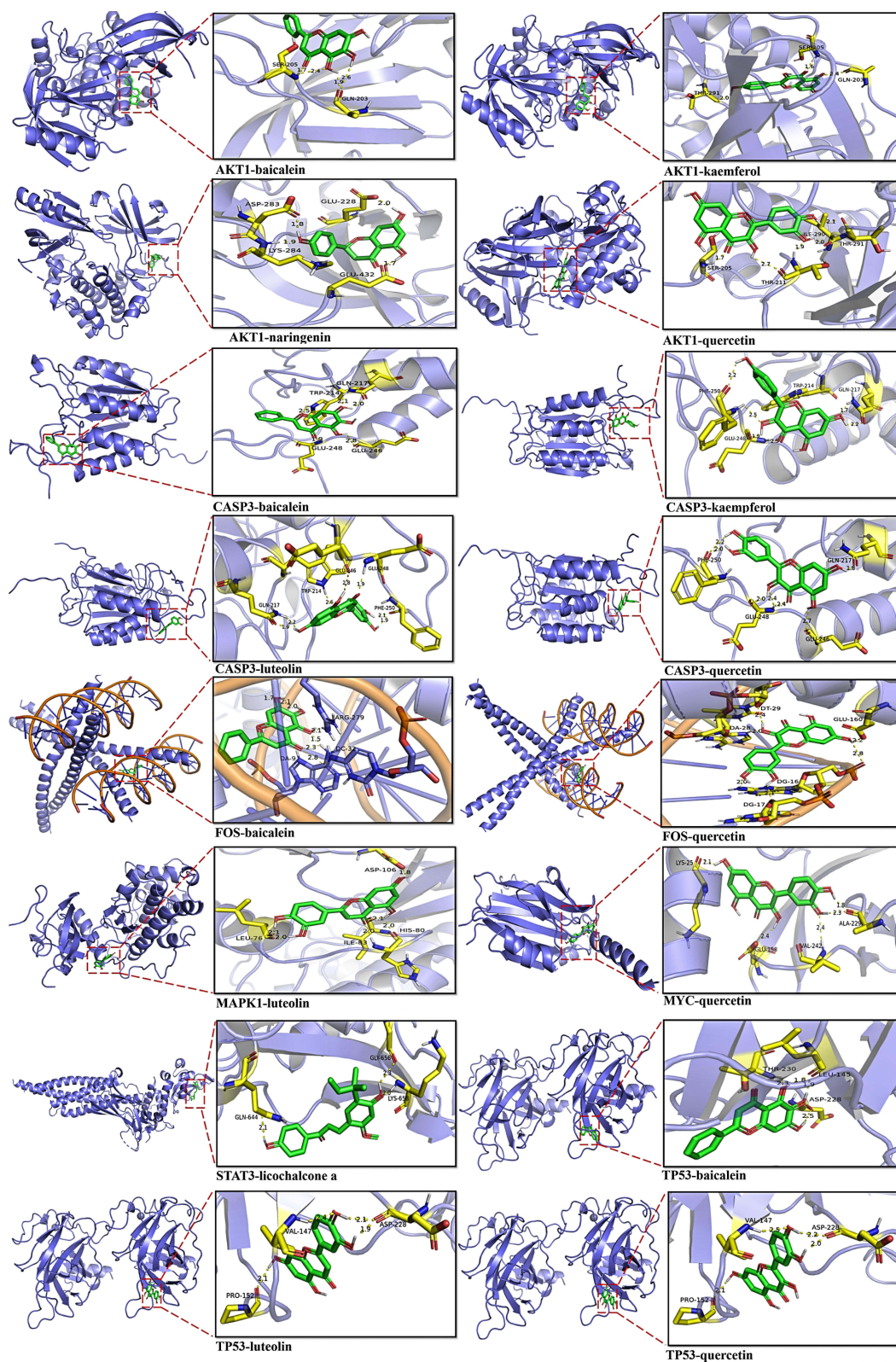
Figure 6 The results of molecular docking between the core targets and core ingredients.
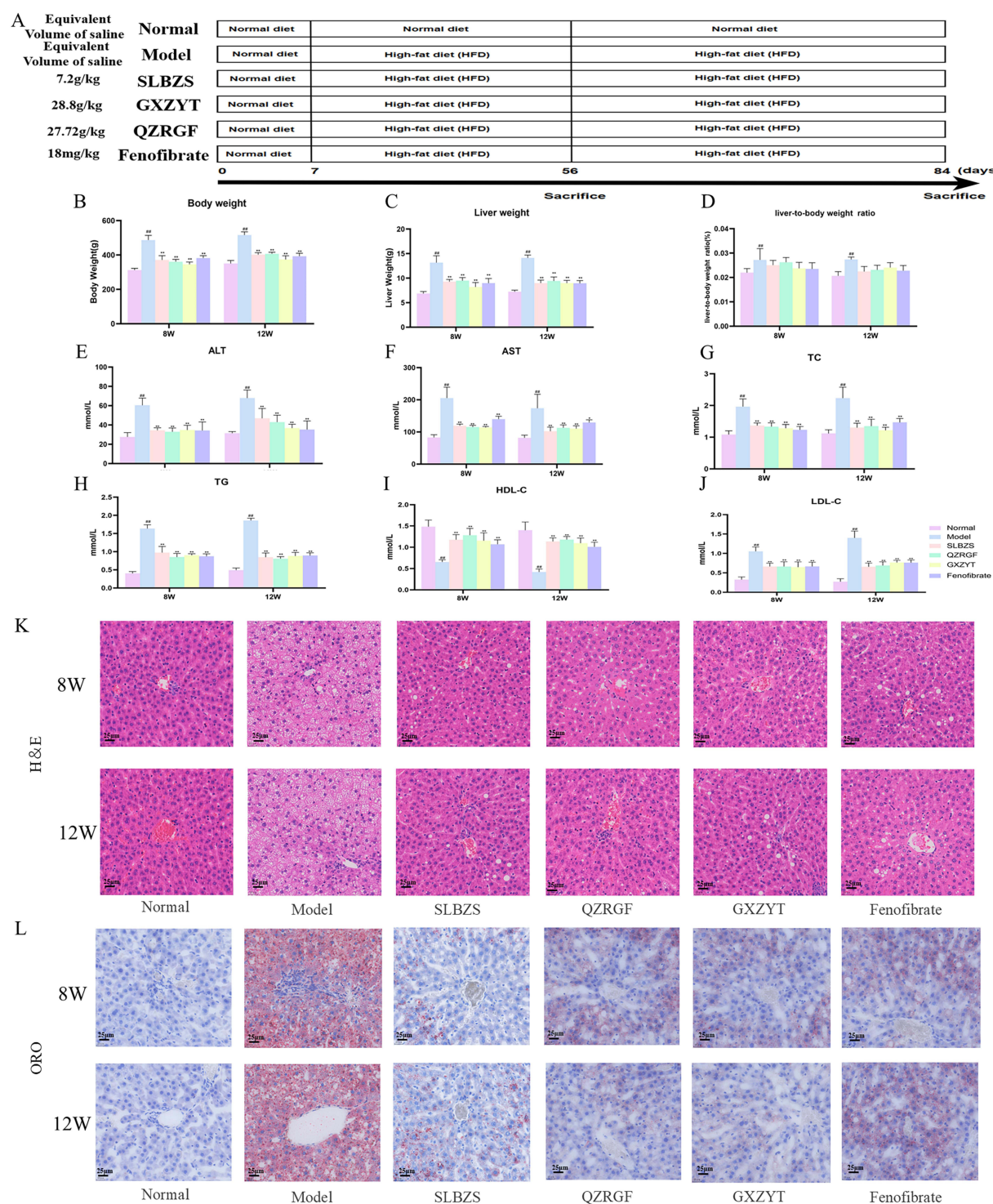
Figure 7 Experimental validation results in NAFLD rats. (**A**) Overall course of animal experiments (**B**) Comparison of body weight of rats in each group (n = 6). (**C**) Comparison of liver weight of rats in each group (n = 6). (**D**) Comparison of liver-body ratios of rats in each group (n = 6). (**E**) Comparison of ALT in rats of each group (n = 6). (**F**) Comparison of AST in rats of each group (n=6). (**G**) Comparison of TC of rats in each group (n=6). (**H**) Comparison of TG in each group (n=6). (**I**) Comparison of HDL-C in rats of each group (n=6). (**J**) Comparison of LDL-C in rats of each group (n=6). (**K**) Pathological staining of rat liver in each group (HE staining, 400×). (**L**) Pathological staining of rat liver in each group (Oil Red O staining, 400×). ##$P < 0.01$, Compared with Normal; *$P < 0.05$, **$P< 0.01$, compared with Model.

flora of the Normal group was gradually separated from that of the other groups of rat in 8W and 12W, and that there was no overlap between the drug-intervention group and the Normal group but there was a tendency for them to be close to each other, and that the SLBZS group was the closest to the Normal group, followed by the GXZYT group. The SLBZS
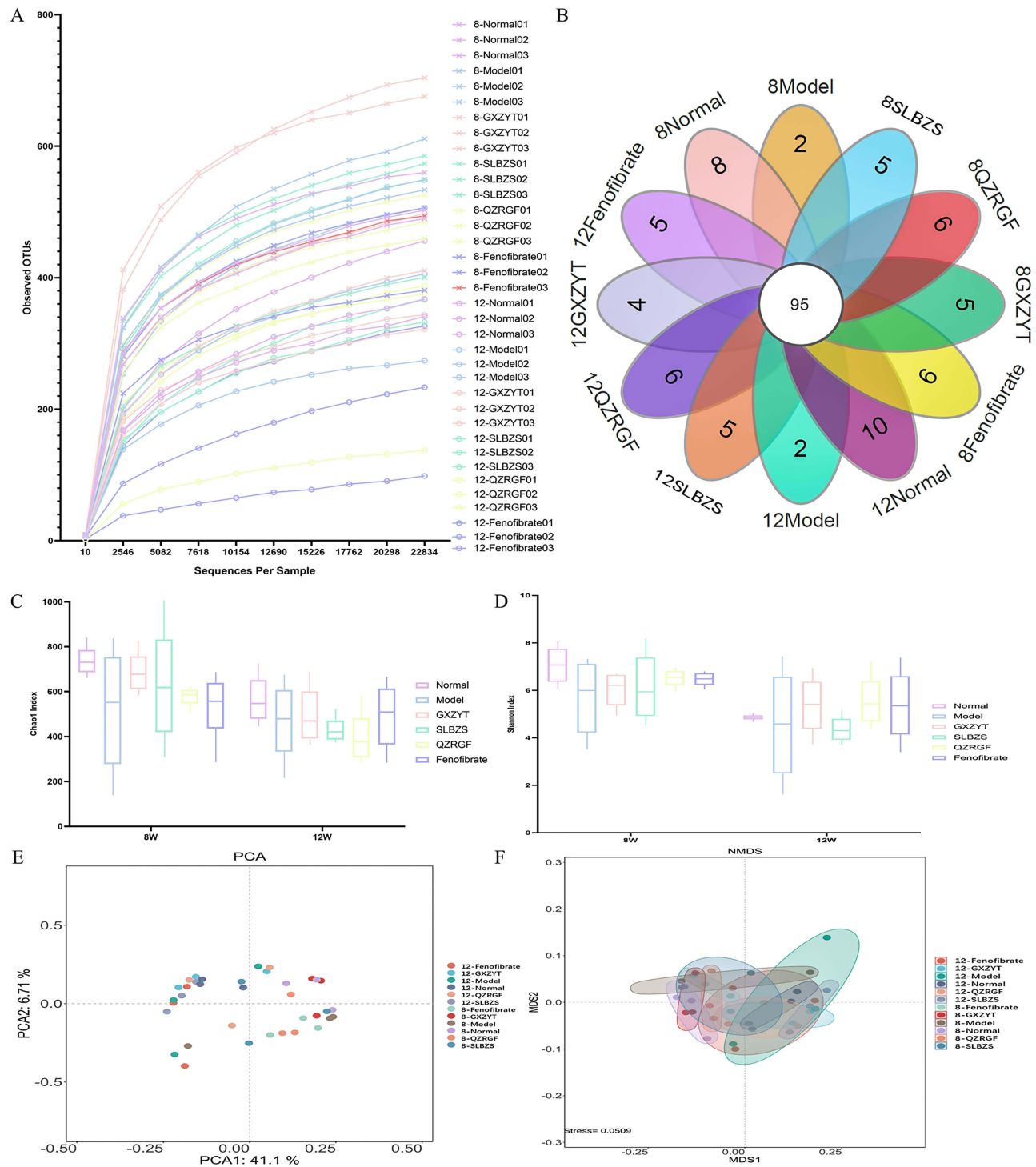
Figure 8 Effect of SLBZS, QZRGF and GXZYT on colony structure in NAFLD rats: (**A**) Dilution curve of community richness of rat intestinal flora in each group (**B**) OTU petal plot of microbial species (**C**) Chao1 index of rat intestinal flora in each group (**D**) Shannon index of rat intestinal flora in each group (**E**) PCA analysis of rat intestinal flora in each group (**F**) MDS analysis of rat intestinal flora in each group.

group was the closest to the Normal group, followed by the GXZYT group and the QZRGF group (Figure 8E). MDS analysis revealed that the intestinal flora of the Normal group and the other groups of rat were also gradually separated in 8W and 12W. Although there was no overlap between the drug intervention group and the Normal group, all drug groups

tended to be close to the Normal group. The SLBZS group was closest to the Normal group, followed by the GXZYT and QZRGF groups (Figure 8F).

Analysis of the Effects of SLBZS, QZRGF and GXZYT on the Phylum and Genus Levels of Intestinal Flora in NAFLD Rats

The top 15 species of rat intestinal flora in terms of maximum abundance at the phylum level were selected, and the highest abundance was found in *Firmicutes* and *Bacteroidetes*, which accounted for more than 80% of the total abundance, followed by *Proteobacteria, Actinobacteria*, and *Fusobacteria* (Figure 9A and B). The ratio of abundance of *Firmicutes* to *Bacteroidetes* (ie, F/B value) in each group, we can see that it was significantly higher in the Model group compared with the Normal group, and the F/B ratio was significantly lower after the intervention of Chinese medicine and Fenofibrate (see Figure 9C–E). Among the six groups of samples, *Bacteroidetes, Fusobacteria, Firmicutes*, and *Fusobacteria* were the most significantly different from each other. *Firmicutes*) showed the most significant differences. The highest percentage of *Firmicutes* was found in the Normal group, and the highest percentage of *Bacteroidetes* was found in the Model group. The smaller percentage of bacterial groups in the six groups were *Proteobacteria, Patescibacteria, Epsilonbacteraeota*, and *Verrucomicrobia*; of these, *Proteobacteria* was found in the Normal group, and the highest percentage of *Bacteroidetes* was found in the Model group. *Proteobacteria* are more highly represented in the Normal group, second only to *Bacteroidetes* in molecular evolutionary studies (Figure 9F and G). Phylogenetic inference can reveal the sequence of evolutionary processes of the organism in question and understand the history and mechanisms of biological evolution. In molecular evolutionary research, systematic inference can reveal the sequence of biological evolution processes, understand the history and mechanisms of biological evolution, and construct evolutionary trees based on the differences in bases between sequences at a certain taxonomic level (Figure 9H–J). We constructed an evolutionary tree based on the maximum likelihood method by selecting OTUs corresponding to the genus level, and found that *Bacteroidetes* and *Firmicutes* had the highest proportion and close relationship.

LEfSe Analysis of the Effects of SLBZS, QZRGF and GXZYT on the Intestinal Flora of NAFLD Rats

LEfSe was then performed to identify specific microorganisms associated with pharmacological interventions with LDA>4. The results showed that (Figure 10A–F) the most characterized bacterial phylum was *Firmicutes* and the genus was *Lachnospiraceae_NK4A136_group* in the 8QZRGF compared to the 8GXZYT group, the 8SLBZS compared to the 8QZRGF group, the most characterized bacterial The most characteristic bacterial phylum was *Firmicutes*, genus *Lachnospiraceae*; 8QZRGF compared with 8GXZYT group, the most characteristic bacterial phylum was *Firmicutes*, genus *Lachnospiraceae_NK4A136_group*; 12QZRGF compared with 12GXZYT group, the most characteristic bacterial phylum was *Helicobacter*, genus *Lachnospiraceae_NK4A136_group*; 12QZRGF compared with 12GXZYT group, the most characteristic bacterial phylum was *Helicobacter*, genus *Helicobacter*. 12SLBZS compared to 12QZRGF group, the most characterized bacterial phylum is *Firmicutes*, genus *weissella*. 12QZRGF compared to 12GXZYT group, the most characterized bacterial phylum is *Firmicutes*, genus *Lachnospiraceae_NK4A136_group*.

Finally, functional prediction analyses based on the homology clustering (COG) family information of the proteome and the Kyoto Encyclopedia of Genes and Genomes (KEGG) homology (KO) information revealed that these cellular functions play a key role in the statistical differences in the composition of the diversity of the phyla, which involve function unknown, posttranslational modification, and the most characteristic bacterial phylum is Firmicutes. posttranslational modification, protein turnover, chaperones, cell motility, transcription, lipid transport and metabolism, carbohydrate transport and metabolism. It indicates that exploring the mechanism of herbal compounding for the treatment of NAFLD in terms of the interrelationships between bacterial flora and signal transduction is a feasible strategy. PICRUST2 was used for KEGG pathway analysis of the intestinal microbiota based on 16S rDNA gene amplicon sequencing results.[53] Cluster analysis of the KEGG pathway at the first level showed that the function of the gut flora in the Model group was mainly in cellular processes and environmental information processing. In contrast, the functions of the gut microbiota in the Medicated group were mainly reflected in human diseases, biological systems, metabolism and genetic information processing (Figure 10G and H).
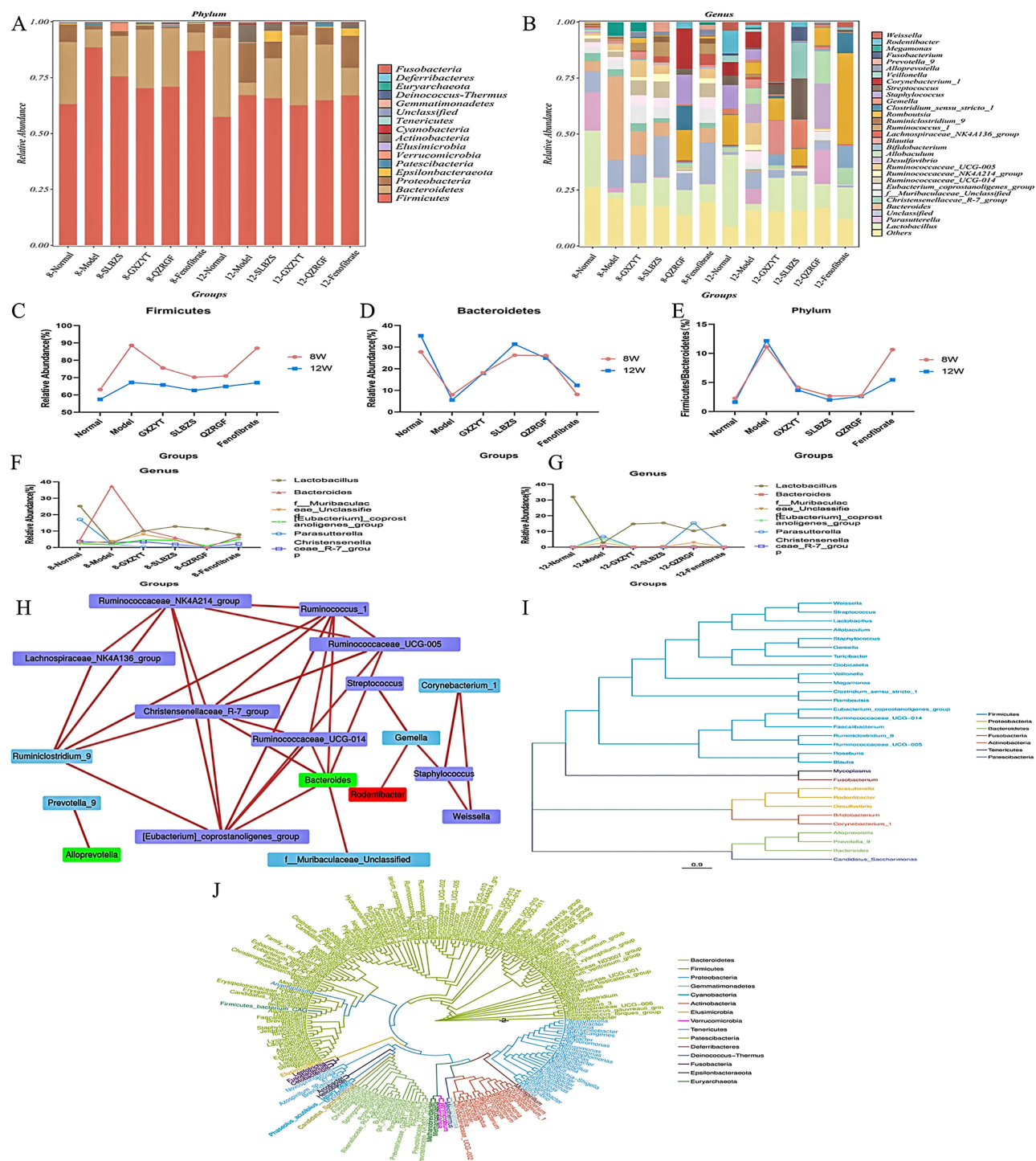
Figure 9 Effects of SLBZS, QZRGF and GXZYT on the levels of intestinal flora phylum and genus in NAFLD rats: (**A**) Percentage of horizontal abundance of rat intestinal bacterial phylum in each group (**B**) Percentage of horizontal abundance of rat intestinal bacterial genus in each group (**C**) Percentage of abundance of thick-walled bacterial phylum in each group (**D**) Percentage of abundance of anaplasmosis phylum in each group (**E**) Percentage of abundance of thick-walled bacterial phylum in each group of rat intestinal phylum/anaplasmosis phylum abundance ratio (F/B)(**F**) 8W Comparison of the top 6 bacterial genera ranked by the relative abundance in the rat intestinal tract in each group (**G**) 12W Comparison of the top 6 genera ranked by relative abundance in the rat intestine in each group (**H**) Network network analysis of rat intestinal flora in each group (**I**) Species evolution tree at genus level of rat intestinal flora in each group (**J**) Phylogenetic evolution tree of rat intestinal flora in each group.
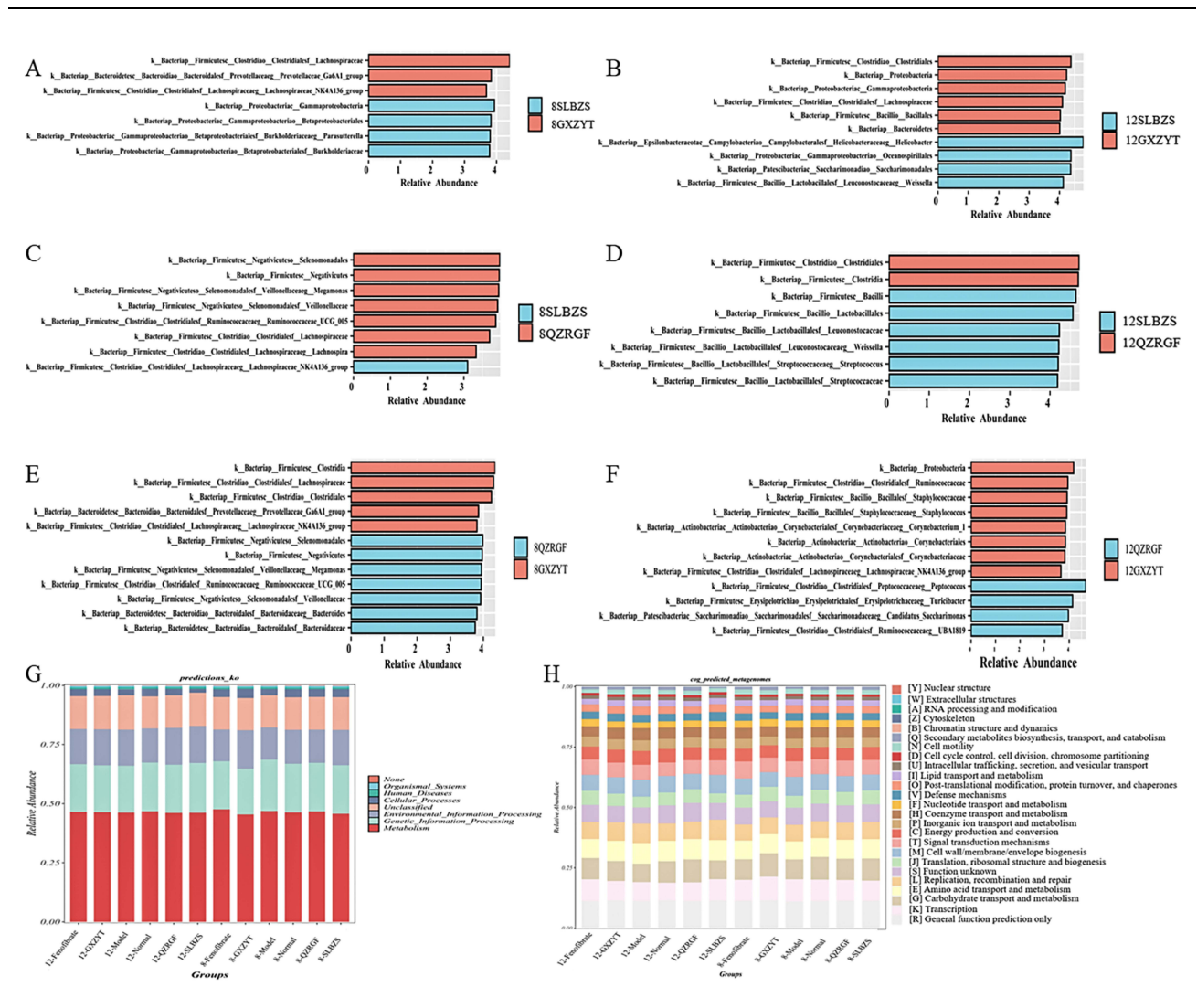
Figure 10 LEfSe analysis showing biomarkers of SLBZS, QZRGF and GXZYT gut microbiota, LDA>4. (**A**) LEfSe analysis of the intestinal flora of 8SLBZS and 8GXZYT rats (**B**) LEfSe analysis of the intestinal flora of 12SLBZS and 12GXZYT rats (**C**) LEfSe analysis of the intestinal flora of 8SLBZS and 8QZRGF rats (**D**) LEfSe analysis of the intestinal flora of 12SLBZS and 12QZRGF rats (**E**) LEfSe analysis of the intestinal flora of 8QZRGF and 8GXZYT rats (**F**) LEfSe analysis of the intestinal flora of 12QZRGF and 12GXZYT rats (**G**) Columnar distribution of KEGG functional abundance of the intestinal flora of the rats in each group (**H**) Columnar distribution of the functional abundance of the intestinal flora of COG in each group of rats.

Note: Taxonomic units are denoted as p (phylum), c (class), o (order), f (family), g (genus) and s (species).

Discussion

Early NAFLD has spleen deficiency, and as the disease progresses, it gradually manifests as blood stasis and phlegm stasis, SLBZS treats spleen deficiency, GXZYT treats phlegm stasis and phlegm stasis; QZRGF softens the liver and strengthens the spleen, regulates qi and promotes blood circulation. The efficacy of each of them has its own focus, so the three parties were selected for the study. SLBZS[21] consists of Dangshen, Fulin, Baizhu, Shanyao, Lianzi, Baibiandou, Yiyiren, Sharen, Jiegeng, Gancao; GXZYT consists of Danggui, Chishao, Chuanxiong, Taoren, Honghua, Wulingzhi, Danpi, Xiangfu, Wuyao, Zhike, Yanhuosuo, Gancao; QZRGF consists of Ezhu, Qingpi, Juhua, Baizhu, Shanzha, Lanhuashen, Sanqi. It was found[54] that Fulin and Baizhu have anti-inflammatory and intestinal flora regulating effects. Taoren, Honghua, Zhike and Yanhusuo are capable of anti-inflammatory and antioxidant in order to protect the liver.[55–58] Wulingzhi,[59] Salvinorin,[60] Xiangfu,[61] Wuyao,[62] Fulin,[63] Gancao,[63] Shanyao,[64] Baizhu polysaccharide,[65] Baizhu lactone,-[66] Ginsenosides,[67] Shanyao polysaccharides,[68] Chishao,[69] Danggui,[70] Jiegeng,[71] Lianzi,[72] Qingpi,[73] Sanqi,[74] Shanzha[75] have found improvements in both gut flora. Acacetin[76] can regulate the composition of intestinal flora, including increasing the content of probiotics and decreasing the content of harmful bacteria. Kaempferol[77] can, at the genus

level, the relative abundance of the genera *Anabacterium spp*. and *Lactobacillus spp*. Luteolin[78] can increase the abundance of the genera of HFD rats *Parvibacter, Faecalitalea, Allobaculum sp*. and *Bacteroids dorei* relative abundance. Naringin, quercetin, baicalin, diosgenin, and licochalcone aincrease the diversity of intestinal flora and improve the abundance of beneficial flora.[79–83] Nobiletin[84] can improve intestinal permeability affecting the composition of the intestinal flora in models of intestinal disorders. AKT1,[85] CASP3,[86] FOS[87] can improve the intestinal flora, enhance the mucosal barrier function and significantly increase the abundance of beneficial bacteria. The MAPK signaling pathway has been associated with the maintenance of intestinal microbial homeostasis.[88,89] The intestinal MYC[90] is involved in the regulation of systemic metabolism and improves hepatic steatosis and steatohepatitis induced by high-fat diet. Expression of STAT3[91] protects the intestinal mucosal barrier and alleviates intestinal flora imbalance. TP53[92] is a key target for improving intestinal flora dysbiosis, and is closely associated with the production of SCFAs and improving inflammatory responses. We focused on the intersecting core targets of SLBZS, QZRGF and GXZYT for the treatment of NAFLD as MAPK1, AKT1, CASP3, FOS, TP53, STAT3, and MYC through the study of network pharmacology; and the core constituents as baicalein, luteolin, nobiletin, quercetin, kaempferol, naringenin, licochalcone a, diosgenin, acetin. Molecular docking of core targets and core components validated the results of the network pharmacology screening. Based on the molecular docking results, affinity < - 7.0 kcal-mol-1 indicates strong docking activity.[52] We targeted AKT1- diosgenin (−9.51), AKT1- kaempferol (−7.38), AKT1- luteolin (−7.48), AKT1- quercetin (−7.4), CASP3- luteolin (−7.11), TP53- baicalein (- 8.41), TP53- luteolin (−8.48), TP53- nobiletin (−7.99), TP53- quercetin (−8.33). Among them, AKT1- diosgenin had the best docking activity. Therefore, we speculate that the core target AKT1, the active ingredient diosgenin may play an important role in the treatment of NAFLD.

According to traditional Chinese medicine theory, the large intestine is the organ of conduction, and its function depends on the liver's ability to relieve stress. The liver and large intestine can be connected through the lung meridian, further demonstrating that the liver and large intestine are interconnected.[93] In his book the Chinese Ming Dynasty physician Li Fu proposed the theory of "Zangfu (Viscera) Connectedness", which states: "The heart is connected to the gallbladder, the liver is connected to the large intestine, the spleen is connected to the small intestine, the lungs are connected to the bladder, the kidneys are connected to the Sanjiao, and the kidneys are connected to the Mingmen". He also proposed[94] the treatment idea of "the liver is connected to the large intestine, and liver diseases should be unblocked from the large intestine". With the concept of "the gut-liver axis" proposed, the association between the occurrence and development of NAFLD and gut microbiota has gradually attracted attention. Numerous studies have shown that gut microbiota plays an important role in the occurrence, development, and treatment of NAFLD.[95] Factors such as intestinal blood influx promote the occurrence and development of NAFLD;[96] Previous studies have shown that beneficial bacterial strains such as lactobacilli can alleviate symptoms of NAFLD by regulating body metabolism, reducing inflammatory responses, and restoring gut microbiota disorders.[97,98]

Clinical data show that the severity of NAFLD is closely related to intestinal dysbiosis, with an increase in the number of potentially pathogenic intestinal bacteria and a decrease in the number of probiotic bacteria, which is accompanied by increased morbidity and morbidity and mortality as the disease progresses in NAFLD.[99] The intestinal flora is involved in an alternating balance of pro- and anti-inflammatory signals, and a compromised intestinal barrier leads to bacterial translocation, which stimulates the hepatic inflammatory response and promotes the progression of NAFLD from simple steatosis to NASH and fibrosis.[100,101] Compared with healthy individuals, the diversity of gut flora was significantly reduced in NAFLD patients, and there were significant alterations in the composition of the gut flora, mainly a significant increase in the abundance of gram-negative bacteria (including *Anaplasma, Aspergillus*, and *Enterobacteriaceae*), and a significant decrease in the abundance of thick-walled phylum of bacteria, especially SCFA-producing bacteria, such as *Lactobacillus*, and *Ruminalococcus*.[102] The present study found that under the intervention of GXZYT, SLBZS and QZRGF the phylum levels *Lactobacillus, Bifidobacterium, Romboutsia, [Eubacterium]_coprosta-noligenes_group, Lachnospiraceae_* increased in relative abundance compared to the model group, while *Bacteroides, Blautia, Ruminococcaceae_UCG-014* decreased in relative abundance compared to the model group. This is in line with other studies of NAFLD through the "gut-liver axis". Jeong Seok Yu et al[103] found that *Lactobacillus* could improve NAFLD progression by modulating the tryptophan pathway in the gut-liver axis. *Bacteroides*, Gram-negative anaerobes in the human and mouse gut microbiota, have been shown to have a variety of beneficial roles, including enhancing the

host mucosal barrier, maintaining immune response homeostasis, and regulating nutrient metabolism.[104] Hu Li et al found[105] that the increased abundance of *Bacteroidetes* was important for ameliorating the metabolic disorders in NAFLD. Dengcheng Hui et al found[106] that Spleen-strengthening and liver-draining formula (SLF) could improve NAFLD by regulating intestinal flora, especially *Lachnospiraceae_NK4A136 group*, and *Ruminococcus* genus to ameliorate NAFLD. Our previous study[22] also confirmed that SLBZS could regulate the intestinal flora of NAFLD rat by increasing the level of beneficial bacteria such as *Lactobacillus* and decreasing the level of *Bacteroides* and *Firmicutes*. Through our study we also found that each group of *Bacteroidetes, Firmicutes* had the highest percentage of genera, and the level of *Firmicutes* showed a decreasing trend and the *Bacteroidetes* showed an increasing trend after the intervention of NAFLD rats by QZRGF, GXZYT and SLBZS. The intervention by GXZYT, SLBZS and QZRGF The relative abundance of the genus levels of *Bacteroidetes, Proteobacteria, Epsilonbacteraeota* and other phyla increased compared to the model group. The relative abundance of *Firmicutes, Actinobacteria, Patescibacteria, Tenericutes* and other bacteria decreased compared to the model group. Xiaoying Yang and her team found that[107] lentinan supplementation may be used to mitigate NAFLD by modulating the microbiota-gut-liver axis. By increasing the abundance of phylum *Actinobacteria* and decreased phylum Proteobacteria and *Epsilonbacteraeota* which is consistent with our 12W results. The interrelationship between bacterial flora and signal transduction was confirmed to explore the mechanism of traditional Chinese medicine compounding for NAFLD as a feasible strategy. The results of our study revealed that SLBZS, QZRGF and GXZYT all had an improving effect on the intestinal flora of NAFLD rats, with SLBZS showing the best improvement. F/B values were significantly decreased after the herbal intervention.

With the continuous research on intestinal flora, it has been found that the dysfunction of intestinal flora has a close relationship with the problem of metabolic diseases. Disturbances in gut flora can promote fatty acid synthesis and monosaccharide absorption, leading to the accumulation of triacylglycerols in adipocytes, which can lead to abnormalities in lipid metabolism and other related symptoms.[108] Disturbances of intestinal flora promote energy absorption by increasing the permeability of the intestine to bacterial products, exacerbate insulin resistance (IR), and promote bacterial translocation in the gut and liver inflammation, which are also important triggers of NAFLD.[109] Lipid metabolism disorders are an important cause of NAFLD, and the liver is an important organ for lipid metabolism in the body[110], and lipid metabolism disorders in the body cause the accumulation of lipids in the liver, which in turn leads to the development of NAFLD. The HFD-induced NAFLD model has been widely used in the study of the prevention and treatment of this disease. The results of a large number of studies have shown that HFD can cause elevated serum TC, TG, LDL-C, ALT, and AST levels in rats and lead to the development of NAFLD.[111,112] Our experiments also confirmed that HFD could lead to a significant increase in serum TC, TG, LDL-C, ALT, and AST ($P<0.01$) and a significant decrease in HDL-C ($P<0.01$) in NAFLD rats, which was significantly decreased after the intervention of SLBZS, GXZYT, and QZRGF. Pathological results of HE and Oil Red O also confirmed that all three parties significantly improved hepatic steatosis. This suggests that all groups of herbal compound can reduce hepatic steatosis and liver injury.

Conclusion

In this study, we investigated the relationship between intestinal homeostasis and hepatic lipid metabolism from the interaction between the intestine and the liver, and preliminarily confirmed that SLBZS, GXZYT and QZRGF have improved the intestinal bacterial flora of NAFLD rats, which provides a basis for combining the theory of traditional Chinese medicine, " Liver and colon association", with the theory of modern medicine, "the gut-liver axis", and explaining the scientific significance of Chinese medicine in the treatment of NAFLD. The combination of the theory of " treat the liver and consolidate the spleen" in TCM and the theory of "the gut-liver axis" in modern medicine provides a basis for explaining the scientific significance of TCM in treating NAFLD.

Although the present study integrates the traditional Chinese medicine concept of "Liver and colon association" and the modern medical concept of "intestinal-liver" axis, it provides a certain basis for the improvement of NAFLD by QZRGF, GXZYT and SLBZS from the perspective of intestinal flora. Using molecular docking technology, it was preliminarily verified that the core targets of QZRGF, GXZYT and SLBZS had strong docking activities with the main active ingredients to improve NAFLD. However, the specific mechanism of action of the three parties to improve NAFLD based on the intestinal flora needs to be further investigated in combination with in vitro and ex vivo

experiments, such as the use of western bolt to verify the expression of the core proteins of the specific pathway of action. As well as in future clinical studies to further validate the effects of tripartite on the intestinal flora of NAFLD patients, and to observe the potential long-term effects, safety and tolerability of the drugs.

Abbreviations

ALT, Alanine aminotransferase; AST, Aspartate aminotransferase; BP, Biological Process; CC, Cell Component; DL, Drug-Likeness; GXZYT, Gexia Zhuyu Tang; GO, Gene Ontology; HDL-C, High-density lipoprotein cholesterol; HE, Hematooxylin-Eosin; KEGG, Kyoto Encyclopedia of Genes and Genomes; LDL-C, Low-density lipoprotein cholesterol; MF, Molecular Function; NAFLD, Nonalcoholic fatty liver disease; OMIM, Online Mendelian Inheritance in Man; OB, Oral Bioavailability; SLBZS, Shenling Baizhu San; QZRGF, Quzhi Ruangan Fang; TC, Total Cholesterol; TCMSP, Traditional Chinese Medicine Systems Pharmacology Database and Analysis Platform; TG, Triglyceride.

Data Sharing Statement

The datasets used and/or analyzed during the current study are available from the corresponding author upon reasonable request Supplementary File.

Ethical Approval and Consent to Participate

This study was approved by the Animal Ethics Committee of Yunnan University of Traditional Chinese Medicine (Ethics Committee approval number: R-062021LH013) following the guidelines for the ethical review of laboratory animal welfare People's Republic of China National Standard GB/T 35892-2018.

Author Contributions

All authors made a significant contribution to the work reported, whether that is in the conception, study design, execution, acquisition of data, analysis and interpretation, or in all these areas; took part in drafting, revising or critically reviewing the article; gave final approval of the version to be published; have agreed on the journal to which the article has been submitted; and agree to be accountable for all aspects of the work.

Funding

Disclosure

The authors declare that they have no conflicts of interest in this study.

References

1. Yang L, Dai Y, He H, et al. Integrative analysis of gut microbiota and fecal metabolites in metabolic associated fatty liver disease patients. *Front Microbiol.* 2022;13:969757. doi:10.3389/fmicb.2022.969757
2. Murag S, Ahmed A, Kim D. Recent epidemiology of nonalcoholic fatty liver disease. *Gut Liver.* 2021;15(2):206–216. doi:10.5009/gnl20127
3. Ratziu V, Bellentani S, Cortez-Pinto H, et al. A position statement on NAFLD/NASH based on the EASL 2009 special conference. *J Hepatol.* 2010;53(2):372–384. doi:10.1016/j.jhep.2010.04.008
4. Jie C, Jialiang C, Kunmin X, et al. Research advances in relationship between nonalcoholic fatty liver disease and inflammatory factors. *Medical Recapitulate.* 2019;25(15):2949–2954. Chinese. doi:10.3969/j.issn.1006-2084.2019.15.007
5. Juanola O, Martínez-López S, Francés R, et al. Non-alcoholic fatty liver disease: metabolic, genetic, epigenetic and environmental risk factors. *Int J Environ Res Public Health.* 2021;18(10):5227. doi:10.3390/ijerph18105227
6. Katsiki N, Mikhailidis DP, Mantzoros CS. Non-alcoholic fatty liver disease and dyslipidemia: an update. *Metabolism.* 2016;65(8):1109–1123. doi:10.1016/j.metabol.2016.05.003
7. Cobbina E, Akhlaghi F. Non-alcoholic fatty liver disease (NAFLD) - pathogenesis, classification, and effect on drug metabolizing enzymes and transporters. *Drug Metab Rev.* 2017;49(2):197–211. doi:10.1080/03602532.2017.1293683

8. Tripathi A, Debelius J, Brenner DA, et al. The gut-liver axis and the intersection with the microbiome. *Nat Rev Gastroenterol Hepatol*. 2018;15 (7):397–411. doi:10.1038/s41575-018-0011-z

9. Ali RO, Quinn GM, Umarova R, et al. Longitudinal multi-omics analyses of the gut-liver axis reveals metabolic dysregulation in hepatitis C infection and cirrhosis. *Nat Microbiol*. 2023;8(1):12–27. doi:10.1038/s41564-022-01273-y

10. Kang SG, Choi YY, Mo SJ, et al. Effect of gut microbiome-derived metabolites and extracellular vesicles on hepatocyte functions in a gut-liver axis chip. *Nano Converg*. 2023;10(1):5. doi:10.1186/s40580-022-00350-6

11. Juneja P, Tripathi DM, Kaur S. Revisiting the gut-liver axis: gut lymphatic system in liver cirrhosis and portal hypertension. *Am J Physiol Gastrointest Liver Physiol*. 2022;322(5):G473–g479. doi:10.1152/ajpgi.00271.2021

12. Zheng Z, Wang B. The gut-liver axis in health and disease: the role of gut microbiota-derived signals in liver injury and regeneration. *Front Immunol*. 2021;12:775526. doi:10.3389/fimmu.2021.775526

13. Csak T, Ganz M, Pespisa J, et al. Fatty acid and endotoxin activate inflammasomes in mouse hepatocytes that release danger signals to stimulate immune cells. *Hepatology*. 2011;54(1):133–144. doi:10.1002/hep.24341

14. Adams DH, Eksteen B, Curbishley SM. Immunology of the gut and liver: a love/hate relationship. *Gut*. 2008;57(6):838–848. doi:10.1136/gut.2007.122168

15. Buzzetti E, Pinzani M, Tsochatzis EA. The multiple-hit pathogenesis of non-alcoholic fatty liver disease (NAFLD). *Metabolism*. 2016;65 (8):1038–1048. doi:10.1016/j.metabol.2015.12.012

16. Aron-Wisnewsky J, Vigliotti C, Witjes J, et al. Gut microbiota and human NAFLD: disentangling microbial signatures from metabolic disorders. *Nat Rev Gastroenterol Hepatol*. 2020;17(5):279–297. doi:10.1038/s41575-020-0269-9

17. Li X, Wu D, Niu J, et al. Intestinal flora: a pivotal role in investigation of traditional Chinese medicine. *Am J Chin Med*. 2021;49(2):237–268. doi:10.1142/s0192415x21500130

18. Wu-Wen F, Shi-Jun Y, Juan L, et al. Discovery of bioactive compounds and effector substance based on gut microbiota. *Chin Traditional Herbal Drugs*. 2020;51(07):1914–1923. doi:10.7501/j.issn.0253-2670.2020.07.029.Chinese

19. Liu-Yi Y, Xiao-Jin L, Qing-Sheng Y, et al. Research progress on Chinese materia medica intervening intestinal flora to improve intestinal mucosal barrier function. *Chin Traditional Herbal Drugs*. 2018;49(08):1932–1938. doi:10.7501/j.issn.0253-2670.2018.08.030.Chinese

20. Yizhu W. Study on prevention and treatment mechanism effect of Scutellaria against alcoholic fatty liver disease based on the gut microbiota and the intestinal mucosal barrier. *Changchun University Chinese Med*. 2023. Chinese. doi:10.26980/d.cnki.gcczc.2023.000339

21. Bo W, Song W, Jun X. Clinical efficacy of Shenling Baizhu powder combined with moving cupping along meridians in treatment of obesity with spleen deficiency and dampness stagnation: a report of 55 cases. *HUNAN J TRADITIONAL CHINESE MED*. 2017;33(07):9–11. Chinese. doi:10.16808/j.cnki.issn1003-7705.2017.07.004

22. Yao Z, Guo J, Du B, et al. Effects of Shenling Baizhu powder on intestinal microflora metabolites and liver mitochondrial energy metabolism in nonalcoholic fatty liver mice. *Front Microbiol*. 2023;14:1147067. doi:10.3389/fmicb.2023.1147067

23. Yao B, Wenjun H, Zheng Y, et al. Experimental research of Quzhi Ruan'gan prescription in effect of vonWillebrand factor in rats with fatty liver caused by high fat. *Chin Med Herald*. 2014;11(01):4–6. Chinese.

24. Ge-Ge T, En-Rui X, Su-Yan Z, et al. Effect of Quzhi Ruangan decoction on TLR4 /NF- κB pathway in rats with nonalcoholic steatohepatitis. *Lishizhen Med Materia Medica Res*. 2023;34(01):77–80. Chinese. doi:10.3969/j.issn.1008-0805.2023.01.19

25. Yinhua Y, Jianing W, Xue H, et al. Haemorheological changes in rats with early-stage non-alcoholic fatty liver disease and the interventional effect of Gexia Zhuyu Tang. *China Pra Med*. 2015;10(05):278–279. Chinese. doi:10.14163/j.cnki.11-5547/r.2015.05.200

26. Xiaosong Z, Tao F, Wenhui C, et al. Effects of Gexia Zhuyu Decoction on lipid metabolism and platelet activation in rats with non-alcoholic fatty liver disease. *Chin Med Herald*. 2016;13(33):4–7+197. Chinese.

27. Rui S. Study on the effect of Shenlingbaizhu powder on liver metabolomics of rats with nonalcoholic fatty liver[master's thesis]. 2020. doi:10.27460/d.cnki.gyzyc.2020.000091. Chinese.

28. Hang Y. Study on the Mechanism of Gexia Zhuyu Decoction In Preventing and Treating Metabolic Associated Fatty Liver Disease By Inhibiting S1P-related Inflammatory Reaction [master's thesis]. 2023. doi: 10.27460/d.cnki.gyzyc.2023.000220. Chinese.

29. Yan C. Metabolomics was used to study the mechanism of QZRGF in the prevention and treatment of rat NAFLD [master's thesis]. 2020. Chinese.

30. Yan R, Yan-Jun D, Han-Bin M, et al. Research progress and challenges of network pharmacology in field of traditional Chinese medicine. *Chin Traditional Herbal Drugs*. 2020;51(18):4789–4797. Chinese. doi:10.7501/j.issn.0253-2670.2020.18.024

31. Hai-Bin C, Hong-Guang Z, Wen-Ting L, et al. Network pharmacology: a new perspective of mechanism research of traditional Chinese medicine formula. *China J Tradition Chinese Med Pharm*. 2019;34(07):2873–2876. Chinese.

32. Li S, Fan TP, Jia W, et al. Network pharmacology in traditional Chinese medicine. *Evid Based Complement Alternat Med*. 2014;2014 (1):138460. doi:10.1155/2014/138460

33. Ru J, Li P, Wang J, et al. TCMSP: a database of systems pharmacology for drug discovery from herbal medicines. *J Cheminform*. 2014;6(1):13. doi:10.1186/1758-2946-6-13

34. Liu Z, Guo F, Wang Y, et al. BATMAN-TCM: a bioinformatics analysis tool for molecular mechANism of traditional Chinese medicine. *Sci Rep*. 2016;6(1):21146. doi:10.1038/srep21146

35. Cai L, Kang YJ. Cell death and diabetic cardiomyopathy. *Cardiovasc Toxicol*. 2003;3(3):219–228. doi:10.1385/ct:3:3:219

36. Qing X, Chunquan Z, Jing H, et al. Progress in the study of the chemical composition of Lanhuasheng. *Asia-Pacific Trad Med*. 2015;11(08):33–35. Chinese. doi:10.11954/ytctyy.201508016

37. Bateman A, Martin M-J, Orchard S. UniProt: the universal protein knowledgebase in 2023. *Nucleic Acids Res*. 2023;51(D1):D523–d531. doi:10.1093/nar/gkac1052

38. Yisong Z, Pan X, Haibo S, et al. Online human Mendelian inheritance database (OMIM). *Mol Cardiol China*. 2001;01:49–51. Chinese. doi:10.16563/j.cnki.1671-6272.2001.01.010

39. Xianchun D, Huangshi DP. Application of network pharmacology in the study of traditional Chinese medicine formula. *Chinese Pharmacol Bulletin*. 2020;36(03):303–308. Chinese. doi:10.3969/j.issn.1001-1978.2020.03.003

40. Piñero J, Ramírez-Anguita JM, Saüch-Pitarch J, et al. The DisGeNET knowledge platform for disease genomics: 2019 update. *Nucleic Acids Res*. 2020;48(D1):D845–d855. doi:10.1093/nar/gkz1021

41. Stelzer G, Rosen N, Plaschkes I, et al. The GeneCards suite: from gene data mining to disease genome sequence analyses. *Curr Protoc Bioinformatics*. 2016;54(1):1.30.1–1.30.33. doi:10.1002/cpbi.5

42. Szklarczyk D, Gable AL, Lyon D, et al. STRING v11: protein-protein association networks with increased coverage, supporting functional discovery in genome-wide experimental datasets. *Nucleic Acids Res*. 2019;47(D1):D607–d613. doi:10.1093/nar/gky1131

43. Yang M, Chen JL, Xu LW, et al. Navigating traditional Chinese medicine network pharmacology and computational tools. *Evid Based Complement Alternat Med*. 2013;2013:731969. doi:10.1155/2013/731969

44. Tang Y, Li M, Wang J, et al. CytoNCA: a cytoscape plugin for centrality analysis and evaluation of protein interaction networks. *Biosystems*. 2015;127:67–72. doi:10.1016/j.biosystems.2014.11.005

45. Drew HR, Wing RM, Takano T, et al. Structure of a B-DNA dodecamer: conformation and dynamics. *Proc Natl Acad Sci U S A*. 1981;78(4):2179–2183. doi:10.1073/pnas.78.4.2179

46. Zhang Y, Sanner MF. AutoDock CrankPep: combining folding and docking to predict protein-peptide complexes. *Bioinformatics*. 2019;35(24):5121–5127. doi:10.1093/bioinformatics/btz459

47. Trott O, Olson AJ. AutoDock Vina: improving the speed and accuracy of docking with a new scoring function, efficient optimization, and multithreading. *J Comput Chem*. 2010;31(2):455–461. doi:10.1002/jcc.21334

48. Caporaso JG, Kuczynski J, Stombaugh J, et al. QIIME allows analysis of high-throughput community sequencing data. *Nat Methods*. 2010;7(5):335–336. doi:10.1038/nmeth.f.303

49. Crawford PA, Crowley JR, Sambandam N, et al. Regulation of myocardial ketone body metabolism by the gut microbiota during nutrient deprivation. *Proc Natl Acad Sci U S A*. 2009;106(27):11276–11281. doi:10.1073/pnas.0902366106

50. Pruesse E, Quast C, Knittel K, et al. SILVA: a comprehensive online resource for quality checked and aligned ribosomal RNA sequence data compatible with ARB. *Nucleic Acids Res*. 2007;35(21):7188–7196. doi:10.1093/nar/gkm864

51. Klindworth A, Pruesse E, Schweer T, et al. Evaluation of general 16S ribosomal RNA gene PCR primers for classical and next-generation sequencing-based diversity studies. *Nucleic Acids Res*. 2013;41(1):e1. doi:10.1093/nar/gks808

52. Hsin KY, Ghosh S, Kitano H. Combining machine learning systems and multiple docking simulation packages to improve docking prediction reliability for network pharmacology. *PLoS One*. 2013;8(12):e83922. doi:10.1371/journal.pone.0083922

53. Ghannam RB, Techtmann SM. Machine learning applications in microbial ecology, human microbiome studies, and environmental monitoring. *Comput Struct Biotechnol J*. 2021;19:1092–1107. doi:10.1016/j.csbj.2021.01.028

54. Juan S, Yu-Zhu G, Zi-Hui L, et al. Shenling Baizhu San ameliorated murine ulcerative colitis based on TLR4 /NF-κB pathway. *Chin J Immunol*. 2020;36(03):294–298+304. Chinese. doi:10.3969/j.issn.1000-484X.2020.03.008

55. Hui Z, Wei WS, Tian L, et al. Mechanism of Qi-regulation plus Aurantii Fructus in the treatment of non-alcoholic fatty liver disease using the network pharmacology and molecular docking analysis. *Zhejiang J Integrated Trad Chin Western Med*. 2022;32(02):116–121. Chinese.

56. Xiu-Feng G, Rui W, Xiu-Fen Q, et al. Advances in studies on chemical constituents and pharmacological effects of Corydalis Yanhusuo. *Chem Engineer*. 2020;34(03):57–60. Chinese. doi:10.16247/j.cnki.23-1171/tq.20200357

57. Yongjian Z, Kai N, Dezhi T, et al. Research on pharmacological effects of peach kernel. *Liaoning J Trad Chinese Med*. 2015;42(04):888–890. Chinese. doi:10.13192/j.issn.1000-1719.2015.04.087

58. Yong YS, Lili G, Jing Y, et al. Advances in the pharmacological effects of Honghua and its development and applications. *North Hortic*. 2015;05:191–195. Chinese. doi:10.11937/bfyy.201505056

59. Qi Y. Study on compatibility of trogopterus dung and panax ginseng changes in chemical and pharmacological activity in vitro[master's thesis]. Jilin Agricultural University; 2011. Chinese.

60. Yuanqing S, Guiming Y. Effect of salvinorin on Adip /CaMKKβ/AMPK pathway in alcoholic fatty liver in mice. *Chinese Pharmacol Bulletin*. 2020;36(01):80–86. Chinese. doi:10.3969/j.issn.1001-1978.2020.01.017

61. Jia L, Jia H. Effects of nutgrass galingale rhizome flavone on diabetic rats and its influence on the levels of blood sugar, blood fat and antioxidant activity in rats. *ANATOMY RES*. 2017;39(06):437–440+456. Chinese.

62. Rui W, Tiantian B, Lihui X, et al. Baihe Wuyaotang ameliorates NAFLD by enhancing mTOR-mediated liver autophagy. *Chin J Exp Traditional Med Formulae*. 2024;30(07):66–77. Chinese. doi:10.13422/j.cnki.syfjx.20240114

63. Wen-Wu H, Ying P, Meng-Yue W, et al. Regulatory effect of Sijunzi Tang and its single herbs on intestinal flora in rats with spleen deficiency. *Chin J Exp Traditional Med Formulae*. 2019;25(11):8–15. Chinese. doi:10.13422/j.cnki.syfjx.20190847

64. Zhang N, Liang T, Jin Q, et al. Chinese yam (Dioscorea opposita Thunb.) alleviates antibiotic-associated diarrhea, modifies intestinal microbiota, and increases the level of short-chain fatty acids in mice. *Food Res Int*. 2019;122:191–198. doi:10.1016/j.foodres.2019.04.016

65. Wang R, Zhou G, Wang M, et al. The metabolism of polysaccharide from atractylodes macrocephala koidz and its effect on intestinal microflora. *Evid Based Complement Alternat Med*. 2014;2014:926381. doi:10.1155/2014/926381

66. Feng W, Liu J, Tan Y, et al. Polysaccharides from atractylodes macrocephala koidz. ameliorate ulcerative colitis via extensive modification of gut microbiota and host metabolism. *Food Res Int*. 2020;138(Pt B):109777. doi:10.1016/j.foodres.2020.109777

67. Dong WW, Xuan FL, Zhong FL, et al. Comparative analysis of the rats' gut microbiota composition in animals with different ginsenosides metabolizing activity. *J Agric Food Chem*. 2017;65(2):327–337. doi:10.1021/acs.jafc.6b04848

68. Qi-Yu G, Ying-Zheng Z, Ling-Bo Z. The influence of Chinese Yam Polysaccharide on growth performance and intestinal micro flora in Konmin mice. *Chin J Gerontol*. 2015;35(20):5685–5687. Chinese. doi:10.3969/j.issn.1005-9202.2015.20.003

69. Haifeng L, Fang L, Qikai W, et al. Effect of high retention enema with Chishao Chengqi Decoction on intestinal microecological imbalance in patients with liver failure. *Chinese J Integrated Trad Western Med Liver Dis*. 2019;29(01):21–22+37. Chinese. doi:10.3969/j.issn.1005-0264.2019.01.007

70. Leilei W, Ran B, Weiling L. Effect of *Angelica sinensis* extract on related microflora in chronic zczema mice. *Chin J Microecol*. 2023;35(07):750–755+764. Chinese. doi:10.13381/j.cnki.cjm.202307002

71. Yuzhu C. Study on Processing Mechanism and Pharmacodynamics of Lilium brownii Processing Platycodon grandiflorum Based on Microbial and Component Changes [master's thesis]. Heilongjiang Academy Chinese Medicine. 2023. Chinese. doi:10.27126/d.cnki.ghlzy.2022.000088

72. Zhichang Z. Study on Intestinal Regulation andMechanism of Lotus Seed Oligosaccharides Monomer in Mice [master's thesis]. Fujian Agriculture and Forestry University; 2024. doi: 10.27018/d.cnki.gfjnu.2018.000450. Chinese.

73. Wenjing L, Kaimin W, Shaoqiu Z, et al. Effects of walnut green husk and its extract on intestinal morphology, mucosa antioxidant activity and microbial diversity of yellow-feather broilers. *China Animal Husbandry Veterinary Med*. 2021;48(06):2056–2065. Chinese. doi:10.16431/j.cnki.1671-7236.2021.06.018

74. Li W. Effects and mechanism on anti-inflammatory bowel disease of Panax notoginseng saponins mediated by gut microbiota [master's thesis]. Central South University; 2024. doi: 10.27661/d.cnki.gzhnu.2022.005159. Chinese.

75. Huan W, Min W, Zhuqing L, et al. Effect of malt hawthorn probiotic complex on improving intestinal peristalsis and regulating intestinal microflora in constipation rats. *Food Science and Technology*. 2023;48(05):89–96. Chinese. doi:10.13684/j.cnki.spkj.2023.05.013

76. Junyu R. Study on the mechanism of acacetin in alleviating ulcerative colitis in mice[master's thesis]. Shanghai University of Traditional Chinese Medicine; 2023. doi: 10.27320/d.cnki.gszyu.2020.000781. Chinese.

77. Wang T, Wu Q, Zhao T. Preventive effects of kaempferol on high-fat diet-induced obesity complications in C57BL/6 mice. *Biomed Res Int*. 2020;2020(1):4532482. doi:10.1155/2020/4532482

78. Sun WL, Yang JW, Dou HY, et al. Anti-inflammatory effect of luteolin is related to the changes in the gut microbiota and contributes to preventing the progression from simple steatosis to nonalcoholic steatohepatitis. *Bioorg Chem*. 2021;112:104966. doi:10.1016/j.bioorg.2021.104966

79. Wu YX, Yang XY, Han BS, et al. Naringenin regulates gut microbiota and SIRT1/ PGC-1α signaling pathway in rats with letrozole-induced polycystic ovary syndrome. *Biomed Pharmacother*. 2022;153:113286. doi:10.1016/j.biopha.2022.113286

80. Nie J, Zhang L, Zhao G, et al. Quercetin reduces atherosclerotic lesions by altering the gut microbiota and reducing atherogenic lipid metabolites. *J Appl Microbiol*. 2019;127(6):1824–1834. doi:10.1111/jam.14441

81. Jung MA, Jang SE, Hong SW, et al. The role of intestinal microflora in anti-inflammatory effect of baicalin in mice. *Biomol Ther*. 2012;20(1):36–42. doi:10.4062/biomolther.2012.20.1.036

82. Juan H, Wenhui H, Mingxia W, et al. Pharmacological actions of potato tea saponaria. *Hebei Med J*. 2004;01:71. Chinese.

83. Yongxin J, Yu Y, Chunlei Y, et al. Inhibition of Haemophilus parasuis by licochalcone A in vitro and in vivo. *Prog Vet Med*. 2019;40(08):74–79. Chinese. doi:10.16437/j.cnki.1007-5038.2019.08.010

84. Laurindo LF, Santos A, Carvalho ACA, et al. Phytochemicals and regulation of NF-kB in inflammatory bowel diseases: an overview of in vitro and in vivo effects. *Metabolites*. 2023;13(1):96. doi:10.3390/metabo13010096

85. Man DL. The impact of a dysbiotic gut microbiota from a genetic obese child on the expression of miRNAs and genes in colon and liver of germ-free mice[master's thesis]. Shanghai Jiao Tong University; 2020. doi:10.27307/d.cnki.gsjtu.2019.002870. Chinese.

86. Hong Y, Yanping T, Lei Y, et al. Effects of Huoxue Tongiiang Prescription on intestinal flora and cysteineprotease 3/gasdermin E pathway in rats with reflux esophagitis. *Chinese J Integrated Trad Western Med Digestion*. 2022;30(10):701–707+712. Chinese. doi:10.3969/i.issn.1671-038X.2022.10.04

87. Tousen Y, Uehara M, Kruger MC, et al. Effects of dietary fibre and tea catechin, ingredients of the Japanese diet, on equol production and bone mineral density in isoflavone-treated ovariectomised mice. *J Nutr Sci*. 2012;1:e13. doi:10.1017/jns.2012.14

88. Wan YD, Zhu RX, Bian ZZ, et al. Retracted: improvement of gut microbiota by inhibition of P38 mitogen-activated protein kinase (MAPK) signaling pathway in rats with severe acute pancreatitis. *Med Sci Monit*. 2022;28:e937193. doi:10.12659/msm.937193

89. Rabiei N, Ahmadi Badi S, Ettehad Marvasti F, et al. Induction effects of Faecalibacterium prausnitzii and its extracellular vesicles on toll-like receptor signaling pathway gene expression and cytokine level in human intestinal epithelial cells. *Cytokine*. 2019;121:154718. doi:10.1016/j.cyto.2019.05.005

90. Luo Y, Yang S, Wu X, et al. Intestinal MYC modulates obesity-related metabolic dysfunction. *Nat Metab*. 2021;3(7):923–939. doi:10.1038/s42255-021-00421-8

91. Jing Z, Xiaojie G, Yingchao F, et al. Research on the mechanism of Dong's unique acupoints and Dingchen Fuzheng Tang in the improvement of postoperative intestinal flora disorder in patients with gastric cancer. *Western J Trad Chinese Med*. 2023;36(12):1–6. Chinese. doi:10.12174/j.issn.2096-9600.2023.12.01

92. Langlang H, Dispatcher X, Jian'an W, et al. Exploring the mechanism of spleen-strengthening, turbidity-reducing and lipid-regulating formula for the treatment of atherosclerosis combined with intestinal flora dysbiosis based on network pharmacology. *Chinese Traditional Patent Med*. 2022;44(10):3347–3353. doi:10.3969/i.issn.1001-1528.2022.10.054.Chinese

93. Jing M, Tulin L. On the liver and the large intestine are connected. *Shaanxi J Trad Chinese Med*. 2019;40(07):927–930. Chinese. doi:10.3969/i.issn.1000-7369.2019.07.032

94. Zhaojun W, Yunxi J. Theoretical research and application of the theory of "Liver connected with the large intestine". *J Zhejiang Chinese Med University*. 2021;45(04):339–344. Chinese. doi:10.16466/j.issn1005-5509.2021.04.004

95. Leung C, Rivera L, Furness JB, et al. The role of the gut microbiota in NAFLD. *Nat Rev Gastroenterol Hepatol*. 2016;13(7):412–425. doi:10.1038/nrgastro.2016.85

96. Cani PD, Amar J, Iglesias MA, et al. Metabolic endotoxemia initiates obesity and insulin resistance. *Diabetes*. 2007;56(7):1761–1772. doi:10.2337/db06-1491

97. Li X, Xiao Y, Huang Y, et al. Lactobacillus gasseri RW2014 ameliorates hyperlipidemia by modulating bile acid metabolism and gut microbiota composition in rats. *Nutrients*. 2022;14(23):4945. doi:10.3390/nu14234945

98. Werlinger P, Nguyen HT, Gu M, et al. Lactobacillus reuteri MJM60668 prevent progression of non-alcoholic fatty liver disease through anti-adipogenesis and anti-inflammatory pathway. *Microorganisms*. 2022;10(11):2203. doi:10.3390/microorganisms10112203

99. Xu M, Luo K, Li J, et al. Role of intestinal microbes in chronic liver diseases. *Int J mol Sci*. 2022;23(20). doi:10.3390/ijms232012661

100. Kolodziejczyk AA, Zheng D, Shibolet O, et al. The role of the microbiome in NAFLD and NASH. *EMBO Mol Med*. 2019;11(2). doi:10.15252/emmm.201809302

101. Lelouvier B, Servant F, Païssé S, et al. Changes in blood microbiota profiles associated with liver fibrosis in obese patients: a pilot analysis. *Hepatology*. 2016;64(6):2015–2027. doi:10.1002/hep.28829

102. Wang B, Jiang X, Cao M, et al. Altered fecal microbiota correlates with liver biochemistry in nonobese patients with non-alcoholic fatty liver disease. *Sci Rep*. 2016;6(1):32002. doi:10.1038/srep32002

103. Yu JS, Youn GS, Choi J, et al. Lactobacillus lactis and Pediococcus pentosaceus-driven reprogramming of gut microbiome and metabolome ameliorates the progression of non-alcoholic fatty liver disease. *Clin Transl Med*. 2021;11(12):e634. doi:10.1002/ctm2.634

104. Zocco MA, Ainora ME, Gasbarrini G, et al. Bacteroides thetaiotaomicron in the gut: molecular aspects of their interaction. *Dig Liver Dis*. 2007;39(8):707–712. doi:10.1016/j.dld.2007.04.003

105. Li H, Wang XK, Tang M, et al. Bacteroides thetaiotaomicron ameliorates mouse hepatic steatosis through regulating gut microbial composition, gut-liver folate and unsaturated fatty acids metabolism. *Gut Microbes*. 2024;16(1):2304159. doi:10.1080/19490976.2024.2304159

106. Hui D, Liu L, Azami NLB, et al. The spleen-strengthening and liver-draining herbal formula treatment of non-alcoholic fatty liver disease by regulation of intestinal flora in clinical trial. *Front Endocrinol*. 2022;13:1107071. doi:10.3389/fendo.2022.1107071

107. Yang X, Zheng M, Zhou M, et al. Lentinan supplementation protects the gut-liver axis and prevents steatohepatitis: the role of gut microbiota involved. *Front Nutr*. 2021;8:803691. doi:10.3389/fnut.2021.803691

108. Le Chatelier E, Nielsen T, Qin J, et al. Richness of human gut microbiome correlates with metabolic markers. *Nature*. 2013;500(7464):541–546. doi:10.1038/nature12506

109. Abdou RM, Zhu L, Baker RD, et al. Gut microbiota of nonalcoholic fatty liver disease. *Dig Dis Sci*. 2016;61(5):1268–1281. doi:10.1007/s10620-016-4045-1

110. Trefts E, Gannon M, Wasserman DH. The liver. *Curr Biol*. 2017;27(21):R1147–r1151. doi:10.1016/j.cub.2017.09.019

111. Li J, Wang T, Liu P, et al. Hesperetin ameliorates hepatic oxidative stress and inflammation via the PI3K/AKT-Nrf2-ARE pathway in oleic acid-induced HepG2 cells and a rat model of high-fat diet-induced NAFLD. *Food Funct*. 2021;12(9):3898–3918. doi:10.1039/d0fo02736g

112. Zhao H, Gao X, Liu Z, et al. Sodium alginate prevents non-alcoholic fatty liver disease by modulating the gut-liver axis in high-fat diet-fed rats. *Nutrients*. 2022;14(22):4846. doi:10.3390/nu14224846